

Static Model of the Harvey Area

A Report by ODIN Reservoir Consultants

For

Department of Mines, Industry Regulation and
Safety

DMIRS/2018/6



June 2018

LIST OF FIGURES	3
LIST OF TABLES	4
DECLARATION	5
1. EXECUTIVE SUMMARY	6
2. OBJECTIVES	8
3. INTRODUCTION	9
4. REGIONAL SETTING	12
5. STRATIGRAPHY	14
5.1 Analogues and conceptual depositional model	17
5.1.1 Core facies analysis	18
6. RECOMMENDATIONS FOR PALEOSOL FACIES MODELLING	21
7. STATIC MODELLING	27
7.1 Well data	27
7.2 Geophysics and structural concept for the area	28
7.3 Well correlation.....	38
7.4 Petrophysical analysis	40
7.4.1 Review of current log Analysis	40
7.4.2 Gamma ray response.....	40
7.4.3 Shale volume	41
7.4.4 Porosity	41
7.4.5 Revised Permeability.....	41
7.4.6 Sand/Shale distribution	44
7.5 Static modelling software	45
7.6 Data base	46
7.7 Structural modelling.....	46
7.8 3D gridding	47
7.9 Facies modelling.....	48
7.10 Petrophysical modelling.....	50
7.11 Sensitivity and uncertainty analysis	53
8. CONCLUSION	55
9. REFERENCES	57

List of Figures

Figure 3.1: Harvey Location Map showing the area of interest	9
Figure 3.2: ODIN Modelling Workflow.....	10
Figure 4.1: Regional Location Map	13
Figure 5.1: "Break-up" Event	15
Figure 5.2: Late Triassic Climate (After Reference 3)	15
Figure 5.3 Stratigraphy of Perth Basin (Harvey Area within red box) (Zhan, 2014)16	
Figure 5.4: Brahmaputra River as an analogue for the Lesueur Sandstone.....	17
Figure 5.5: Pacific Hwy cutting near Gossford through Triassic Hawkesbury Sandstone. Photo courtesy of J Roestenburg (Roestenburg, 2016).....	18
Figure 5.6: Example of core facies in Harvey-1 (Piane, et al., 2013).....	19
Figure 6.1: Pedogenic development in a fluvial system related to sea-level cycle (Wright & Marriot 1993 in (Kraus, 1999).....	22
Figure 6.2: Different sedimentation rates associated to different small-scale basin conditions (Kraus, 1999).	24
Figure 7.1: Location Map Showing Key Elements and Areas.....	27
Figure 7.2: Seismic Survey Map	28
Figure 7.3: Shows Gaps in Seismic due to acquisition constraints.....	29
Figure 7.4: Fault orientations	30
Figure 7.5: Horizons interpreted with GSWA Harvey 1 well tie	31
Figure 7.6: Top Yalgorup Member Depth Map.....	32
Figure 7.7: Intra Yalgorup Marker 01 Depth Map.....	33
Figure 7.8: Top Wonnerup Member Depth Map.....	34
Figure 7.9: Intra Wonnerup Marker 02 Depth Map.....	35
Figure 7.10: Intra Wonnerup Marker 01 Depth Map.....	36
Figure 7.11: Top Sabina Sandstone Depth Map	37
Figure 7.12: Correlation Panel.....	39
Figure 7.13: Wonnerup Log Derived Total Porosity vs NMR Perm	43
Figure 7.14: Revised Porosity Permeability Transform for Wonnerup.....	43
Figure 7.15: Yalgorup Porosity vs Permeability NMR (Left) & Core (Right).....	44
Figure 7.16: Yalgorup Porosity Permeability Transform.....	44
Figure 7.17: Example of grid dimensions using 'Control Lines' in RMS.....	45
Figure 7.18: 3D View of Fault Surfaces.	46
Figure 7.19: Structural Model with Faults.....	47
Figure 7.20: Grid at 250x250m cell size.....	48
Figure 7.21: Simplified Facies types used in Facies Model.....	49
Figure 7.22: Section Showing the Facies Distribution	49
Figure 7.23: Vertical Proportions for Facies	50
Figure 7.24: Porosity Depth Trend.....	51
Figure 7.25: Section showing porosity distribution.	51
Figure 7.26: Revised Porosity Permeability Transform for Wonnerup.....	52
Figure 7.27: Permeability Distribution – "Reference" Versus "High Perm" Case .	53

List of Tables

Table 1: Summary of ranges/scenarios for injection and/or plume migration 7

Table 2: Summary of ranges/scenarios for injection and/or plume migration 54

Declaration

ODIN Reservoir Consultants was commissioned to undertake to provide a reservoir modelling study for the South West Hub CO₂ Sequestration Project on behalf of the Department of Mines, Industry Regulation and Safety (DMIRS)

The evaluation of Carbon Capture and Storage is subject to uncertainty because it involves judgments on many variables that cannot be precisely assessed, including CO₂ sequestration rates and capture, the costs associated with storing these volumes, sequestration gas distribution and potential impact of fiscal/regulatory changes.

The statements and opinions attributable to us are given in good faith and in the belief that such statements are neither false nor misleading. In carrying out our tasks, we have considered and relied upon information supplied by the DMIRS and available in the public domain. Whilst every effort has been made to verify data and resolve apparent inconsistencies, neither ODIN Reservoir Consultants nor its servants accept any liability for its accuracy, nor do we warrant that our enquiries have revealed all of the matters, which an extensive examination should disclose.

We believe our review and conclusions are sound but no warranty of accuracy or reliability is given to our conclusions.

Neither ODIN Reservoir Consultants nor its employees has any pecuniary interest or other interest in the assets evaluated other than to the extent of the professional fees receivable for the preparation of this report

Note:

ODIN has conducted the attached independent technical evaluation with the following internationally recognised specialists:

Geoff Strachan is a petroleum geologist and specialist Geomodeller with over 20 years of experience in the industry covering a wide range of environments. Geoff has built geological models and provided geological support to evaluate and generate prospects for a drilling campaign. He has also co-ordinated and completed an FDP (Field Development Plan), including building static models and providing input for development well locations. In addition, he has been responsible for co-ordinating the G&G component of several development projects, which also involved evaluating upside potential near the fields and quality control of Fields, Prospects and Leads.

1. EXECUTIVE SUMMARY

ODIN Reservoir Consultants was commissioned by the Department of Mines, Industry Regulation and Safety (DMIRS) to provide a multi-disciplinary group with sub-surface skill sets to:

- 1) Undertake an interpretation of the 3D seismic data;
- 2) provide support through reservoir model building and updating of the South West Hub Project in the southern Perth Basin; and
- 3) provide on-going technical support.

As an integral part of the above, ODIN Reservoir Consultants constructed 3D geological stochastic models of the Harvey area to be used in dynamic models to assess the impact of geological uncertainties on the CO₂ storage process which are necessary to establish the suitability of the Harvey structure to act as a CO₂ storage area.

The Harvey structure, onshore Perth Basin, is a North-South elongated fault bounded anticline. The study area for this project within this structure covers 332km² and is located approximately 13km northwest of the town of Harvey south of Perth. The static model grids built for this study are 10km wide by 12.5km long, covering an area of approximately 125km², are the primary input to the dynamic modelling of CO₂ sequestration in the Harvey Area. The static model study provided a reasonable description of the sub-surface in the Harvey area using the interpreted horizon and faults from seismic. This project also included:

1. Detailed Seismic Interpretation, Log & Petrophysical Property Review.

- The following evaluations were undertaken:
 - Detailed interpretation of reprocessed seismic data, resulting in a large number of faults being identified
 - In-depth evaluation of seismic attributes
 - Petrophysics review of the four available wells and offset wells. With integration of NMR and core data to update the porosity/permeability transform
 - Extensive literature review of paleosols with analogues provided
 - Well correlation panels were prepared for facies, porosity and permeability

2. Static modelling – structure, facies and properties

- The static model construction resulted in various realisations guided by known uncertainty (paleosol continuity, fault definition, reservoir connectivity and reservoir quality).

The key uncertainties identified of the static modelling of the Harvey area are:

- How extensive are the individual paleosol geobodies?
- Porosity versus depth trend
- Permeability range
- Fault seal
- Vertical-to-horizontal permeability ratio
- Impact of upscaling cells for simulation has been accessed

The range of geological uncertainties investigated in the geomodelling study are summarised in Table 1. Geological models representing these ranges were incorporated into dynamic models investigating the movement of the CO₂ plume during injection of CO₂ and subsequent shut-in.

Table 1: Summary of ranges/scenarios for injection and/or plume migration

Parameter	Range (Gen 3 Models)	Range (Gen 4 Models)	Comments
<i>Paleosol Dimensions</i>	500-1500-3500m	300-3000-10000m	Based on an extension literature review and analogues a wider range of paleosol sizes have been used in Gen4.
<i>Permeability range in the Wonnerup</i>	71 to 372mD. Mean = 200mD	0 to 900 mD Mean = 138mD High Perm Case: Mean = 200mD	Significantly reduced permeability based on the NMR interpreted permeability and the porosity versus depth trend used.
<i>Fault Seal</i>	0.1 & 1	0.01 & 1	Open/partially closed system for internal faults.
<i>Fault Permeability</i>	x10	x10	Multiply vertical perm near faults by 10.
<i>Kv/Kh in the Wonnerup</i>	Mean = 0.3 to 1	0.1 x Horizontal & 0.8 x Horizontal Perm	
<i>Seismic Based Case</i>	Additional paleosols.	Reference Case	Seismic based case with higher concentration of paleosols/diagenesis in the Wonnerup.
<i>Homogeneous Case</i>	Reference Case	Homogeneous Reservoir or "Bland" Case	Lower percentage of paleosols in the Wonnerup.

2. OBJECTIVES

The objective of this study is to construct 3D geological stochastic models of the Harvey area to be used in dynamic models to assess the impact of geological uncertainties on the CO₂ storage process to establish the suitability of the Harvey structure to act as a CO₂ storage area.

Firstly, a review of the available literature on the subject at a global scale has been carried out and a number of general geological parameters controlling the process have been established and described within.

Secondly, a 3D static model integrating all geological controlling factors particular to the Harvey area has been built and the uncertainty of such factors evaluated. The 3D model integrates the latest data reviews, interpretations and analysis results carried out by a number of subsurface disciplines as part of the project. These include a detailed seismic/attribute interpretation, petrophysical interpretation and a geomechanical review.

Through this process a general workflow for the Harvey project has been developed while identifying the key uncertainties and recommended future work.

3. INTRODUCTION

The Harvey structure (Figure 3.1) in the southern Perth Basin, which covers an approximate area of 332km², constitutes a potential storage area for CO₂ sequestration. The sandstone rich Wonnerup Member in the Lesueur Formation forms the target injection reservoir, with the containment (based on previous studies) within the same sands of the Wonnerup Member. However, the overlying Yalgorup member, which is represented by the paleosol rich, was assessed in greater detail to reveal its containment potential should the plume migrate vertically into this member.

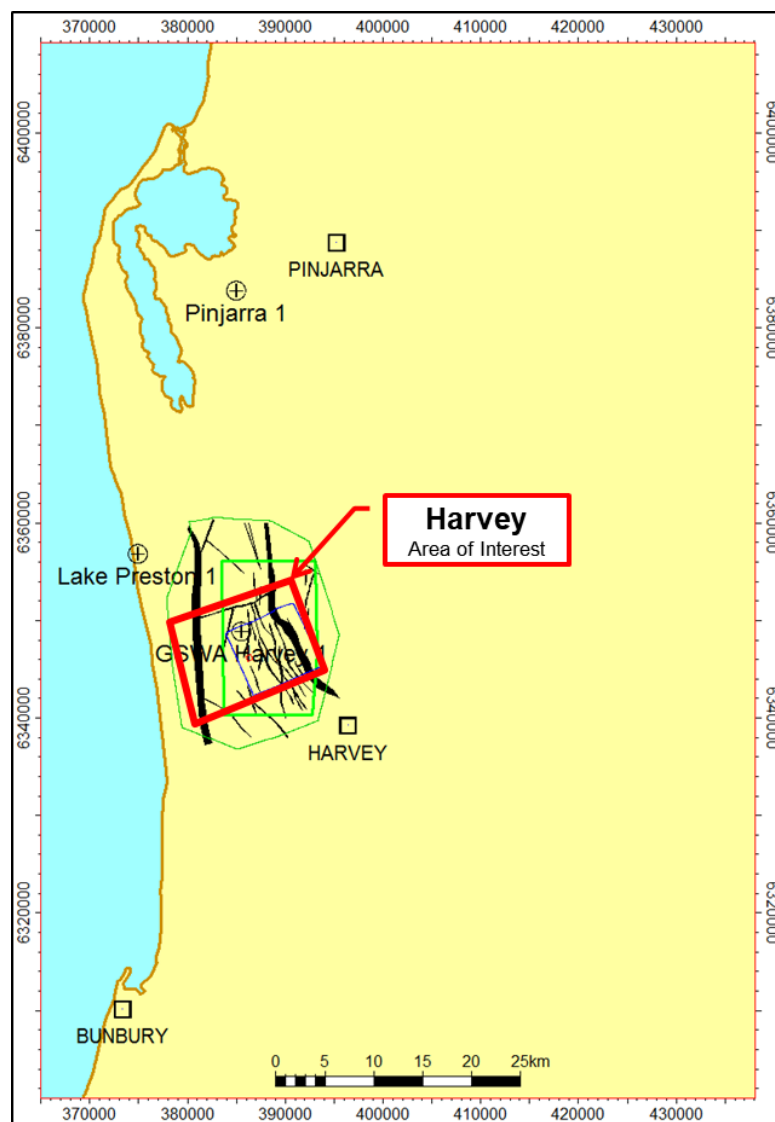


Figure 3.1: Harvey Location Map showing the area of interest

During the first phase of this project a geological report including the general structural geology and sedimentology of the southern Perth basin and the deposition of the Lesueur formation were carried out. Descriptions of the input data their interpretation and use in the building of the 3D static model were also supplied. This report integrates the well and seismic data/interpretations with the knowledge gained from studying analogues in order to define the 3D Geological Model and the distribution of facies/properties (see Figure 3.2). The learnings from the first phase of this project and previous studies have been applied to the study.

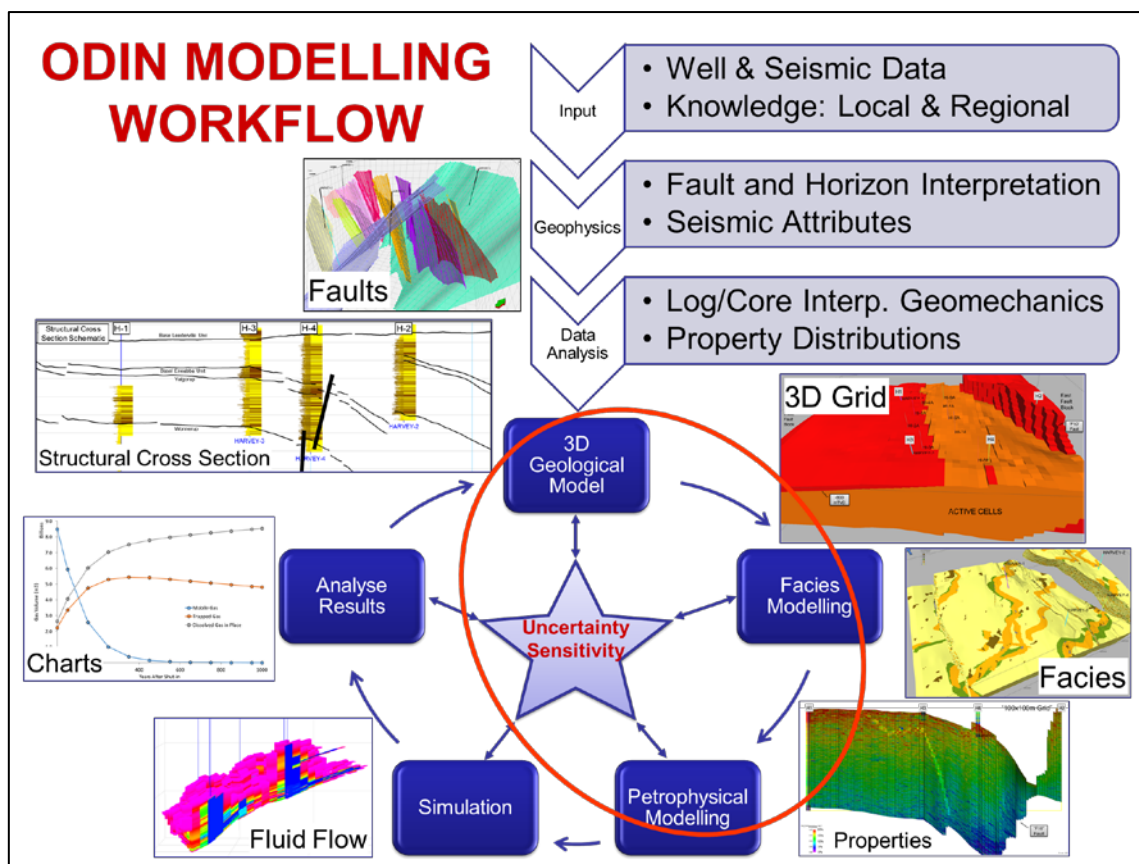


Figure 3.2: ODIN Modelling Workflow

To assess the suitability of a particular site for storage of carbon dioxide, it is necessary to have an adequate geological model and then to use this as the basis for a numerical simulation which can predict the behaviour of the injected carbon dioxide in the subsurface. Unlike a typical oil-field development, the model needs to be simulated not only during the injection phase but also for up to a thousand years after injection, in order to confirm the storage integrity.

3D geological stochastic models allow the assessment of the different geological uncertainties related to the CO₂ storage process which are necessary to establish the suitability of the Harvey structure to act as a CO₂ storage area. The resulting 3D static geomodel will be the base for the assessment of the reservoir engineering parameters that will control the CO₂ sequestration process and determine the ultimate viability of the project.

The main input data used for the 3D Geomodel generation has been the result of all the analysis carried out by other disciplines as part of this project. A summary of the analysis of input data used to build the static model has been included in this report.

4. REGIONAL SETTING

The Perth Basin is a north-south elongate extensional basin stretching along the coastline of Western Australia. It was formed during the separation of Australia and India from the Permian to the Early Cretaceous. A rift complex developed in the area due to extension in a south-west direction during the Permian and Early Triassic. During this stage continental clastic deposits were dominant and widespread.

The extension continued until the Jurassic leading to the generation of a graben and half-graben system in the central part of the basin with marine ingression and deposit of marine sediments. The rift system culminated with the breakup of Gondwana in the Late Cretaceous where dextral transtension dominated the northwest of the basin. There was widespread inversion, erosion, strike-slip tectonics and volcanism.

The Perth Basin is bounded by the N-S Darling Fault and Yilgarn Craton to the East and it extends offshore as far as the continent–ocean boundary to the West. The basin architecture is dominated by listric, extensional, north to north-west trending faults that controlled the distribution of the sediments, compartmentalising the basin into a series of sub-basins. It is considered that sedimentation broadly kept pace with accommodation space during faulting and subsidence.

The study area is located in the onshore part of the southern Perth Basin, Harvey Ridge, between the Mandurah Terrace in the North and the Bunbury Trough in the South. Some studies have suggested that the Harvey Ridge was a result of the northwest–southeast trending transfer movement (Figure 4.1). The “Study Area” marked in Figure 4.1 shows the greater area covered by earlier studies; the area for the Static and Dynamic Models is a much smaller area which is shown in Figure 3.1.

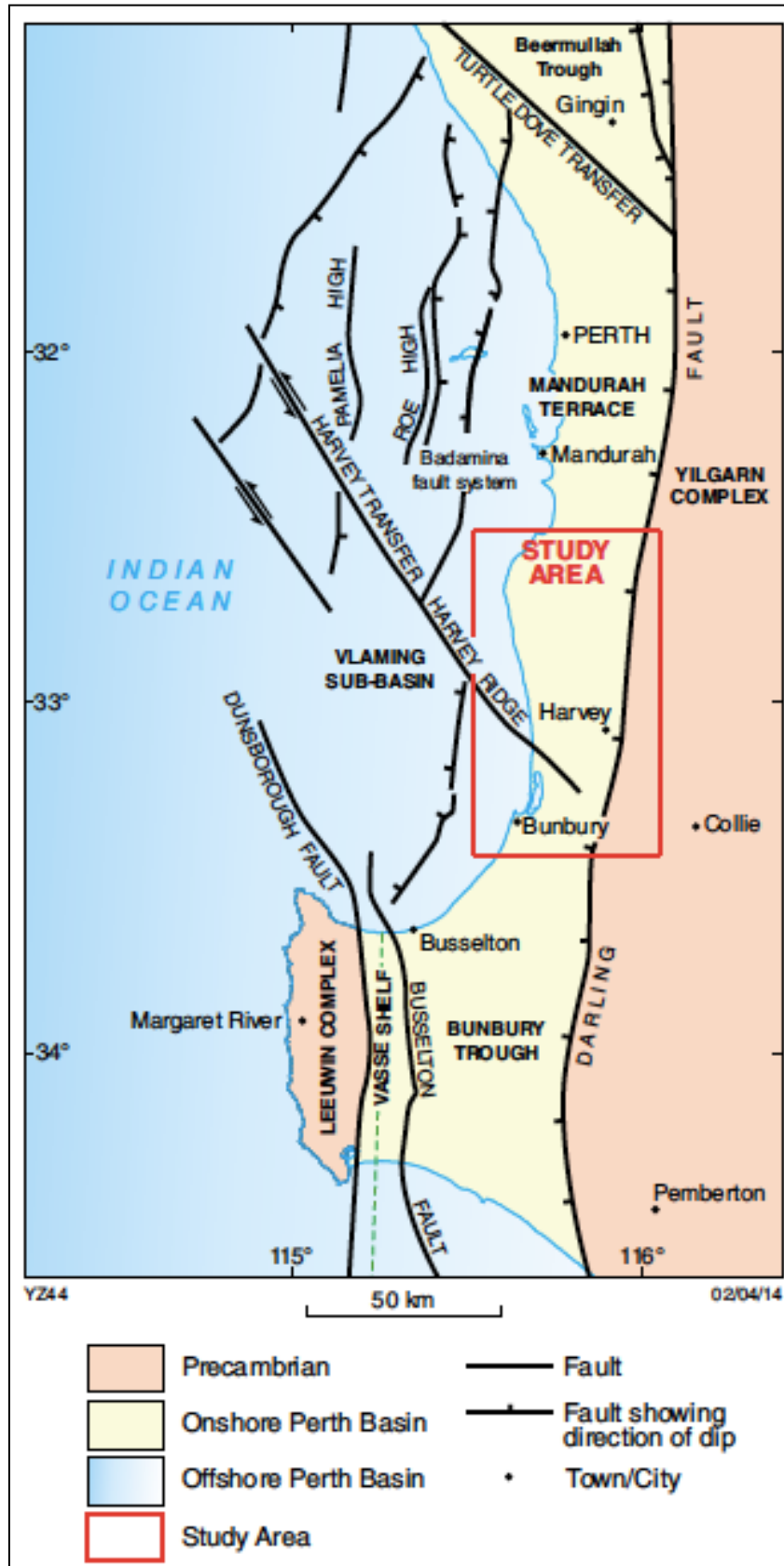


Figure 4.1: Regional Location Map

5. STRATIGRAPHY

The Lesueur Formation was developed in the Perth Basin during the Late Triassic (Figure 5.1 to Figure 5.3). At the time, the basin was undergoing a phase of thermal subsidence because of an initial stage of rifting in the Gondwana supercontinent. This rifting event took place from the late Permian to the Lower Cretaceous when the final break-up of the continent occurred, and the drifting phase of India/Australia began (Figure 5.1)

During the Late Triassic, the global climate was generally warm; there was no ice at either North or South Poles and warm temperate condition extended to the poles. The Perth Basin region was under a warm temperate regime (Figure 5.2). The paleogeography of the basin indicates an elongated shape aligned in an approximately north-south orientation and bounded by stable cratons, which constitute the sediment source.

The Lesueur formation was deposited in a fluvial environment. The two lithostratigraphic members that comprise the Lesueur Formation, Wonnerup Member and Yalgorup Member present some depositional differences. The Wonnerup Member is formed by a fluvial braided system dominated by linguoid bars whereas the Yalgorup Member is formed by a fluvial meandering system dominated by point bars, claystone irregular bodies and paleosols. Five main depositional facies ranging from channel fill sands to swampy over bank deposits have been defined. Paleosol sediments are present in both fluvial environments, braided and meandering, in the Wonnerup and Yalgorup respectively.

In general, the coarse channel fill sands in the Wonnerup Member are a good quality reservoir and the Yalgorup Member is dominated by a more clay rich floodplain and paleosols deposits. The present analogue used for both fluvial systems in the Wonnerup and Yalgorup Members is the Brahmaputra braided river. This example constitutes a good guide to design the modelling parameters of the reservoir formation.

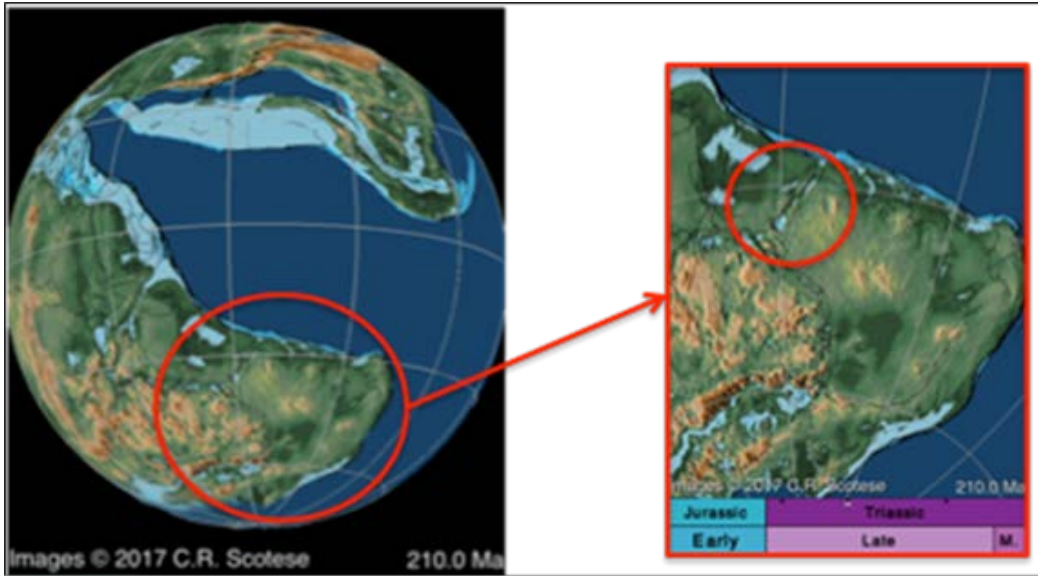


Figure 5.1: "Break-up" Event

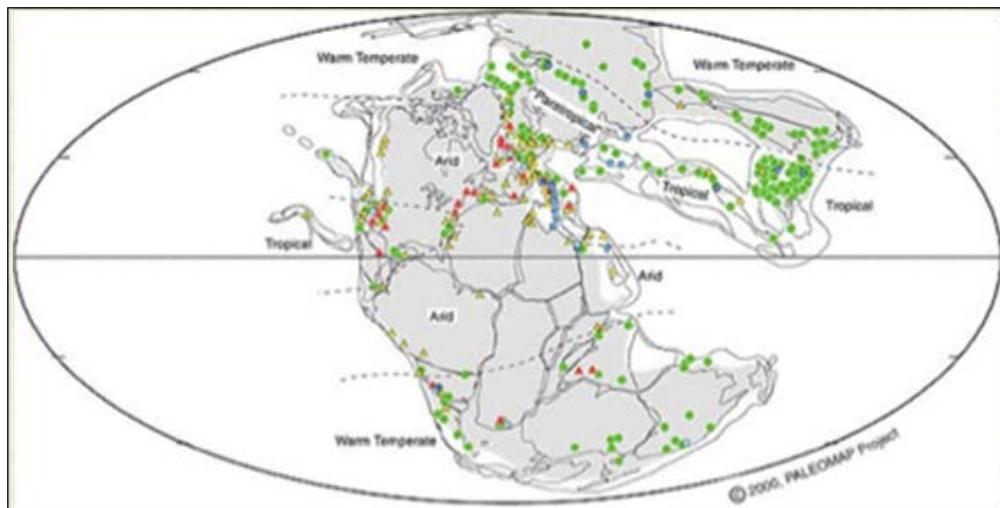


Figure 5.2: Late Triassic Climate (After Reference 3)

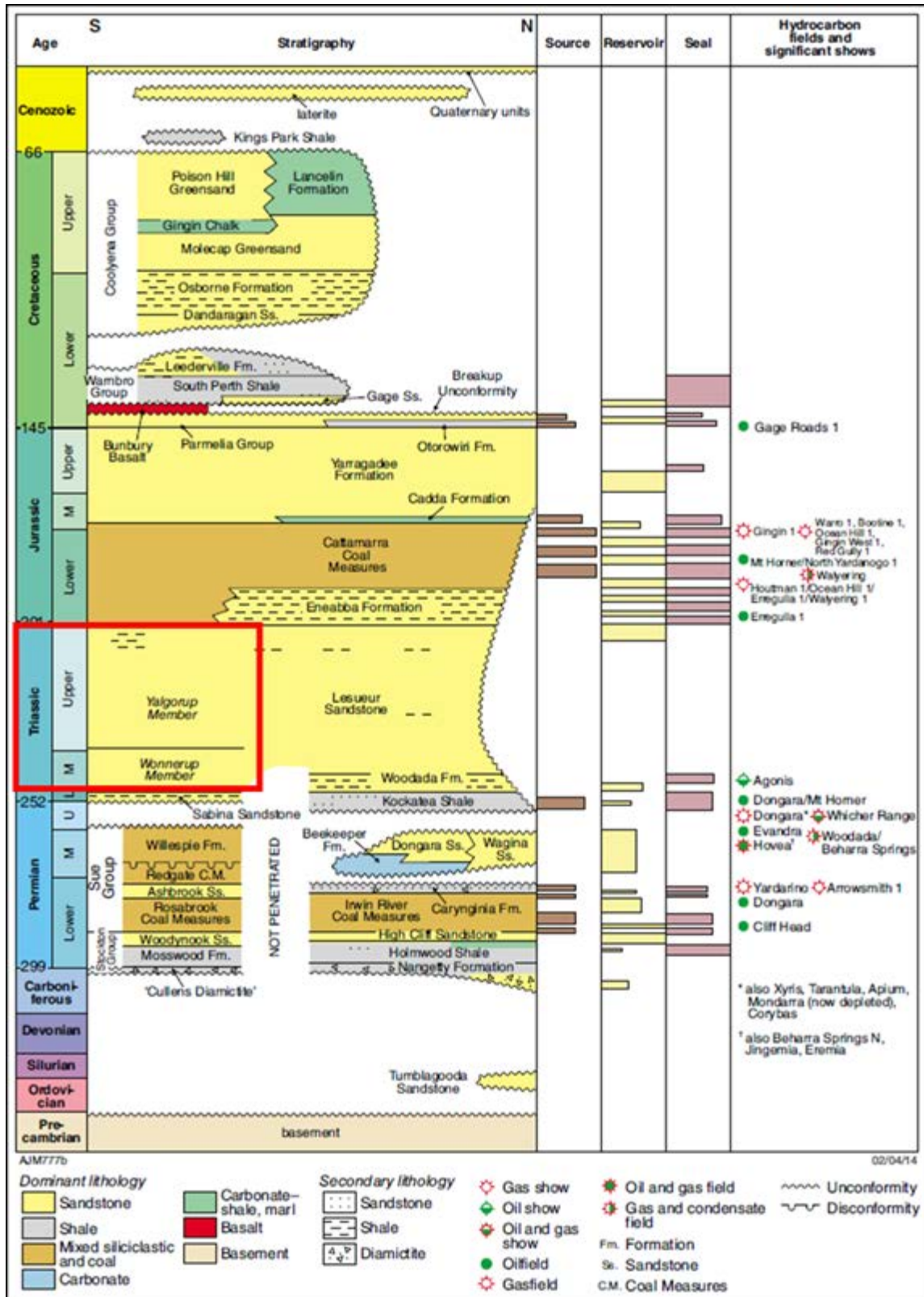


Figure 5.3 Stratigraphy of Perth Basin (Harvey Area within red box) (Zhan, 2014)

5.1 Analogues and conceptual depositional model

The present analogue used for both the Wonnerup member is the Brahmaputra River (Figure 5.4). Other possible analogues for the fluvial environment of the Wonnerup member have also been reviewed, two possible analogues are the Hawkesbury Formation (Figure 5.5) in Eastern Australia and the Durkand Group in the Triassic deposits of USA.

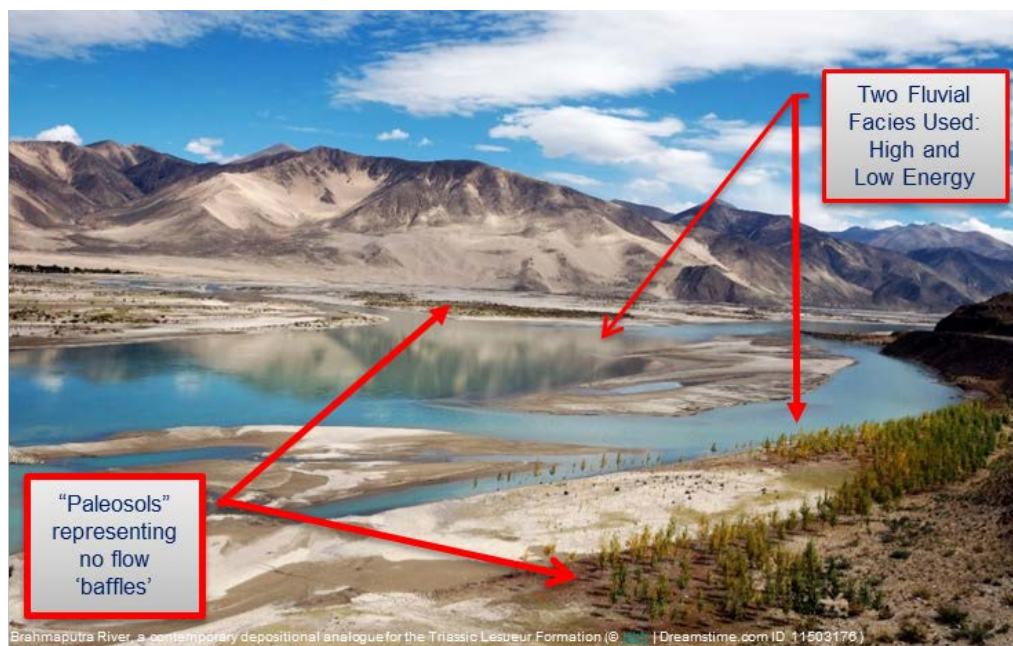


Figure 5.4: Brahmaputra River as an analogue for the Lesueur Sandstone



Figure 5.5: Pacific Hwy cutting near Gossford through Triassic Hawkesbury Sandstone. Photo courtesy of J Roestenburg (Roestenburg, 2016).

5.1.1 Core facies analysis

Nine different lithofacies (Figure 5.6) have been defined over the cored section of Harvey-1 which comprise both the Yalgorup and the Wonnerup members. These nine facies (Ai, Aii, Aiii, B, C, D, E, F, G) have different characteristics in terms of lithology, colour, texture, grain size, sorting, etc. and roughly represent different depositional facies (Piane, et al., 2013).

Ai – High energy channel fill, commonly cross bedded, gravelly to very coarse sandstone.

Aii – High energy fluvial channel barforms, medium to very coarse cross bedded sandstone with significant grain size variation between beds.

Aiii – Fluidized fluvial barforms, massive, coarse sandstone.

B – Moderate energy fluvial barforms, massive, medium sandstone with flaser cross lamination.

C – Moderate to low energy stacked rippleforms, fine to medium cross laminated sandstone, with common organic fragments and flaser-drapes.

D – Floodplain paleosols (often vertisols), fine to medium homogenized sandstone with rootlets, dessication cracks and slickensides.

E – Swampy/lagoonal deposits, under waterlogged conditions, muddy bioturbated sandstone with slumps and dewatering structures.

F – Crevasse splays and overbank deposits, interbedded silty fine sandstone and siltstone with trough cross lamination.

G – Swampy/ overbank deposits, muddy laminated silt with plant fragments and thin laminated fine sandstone.

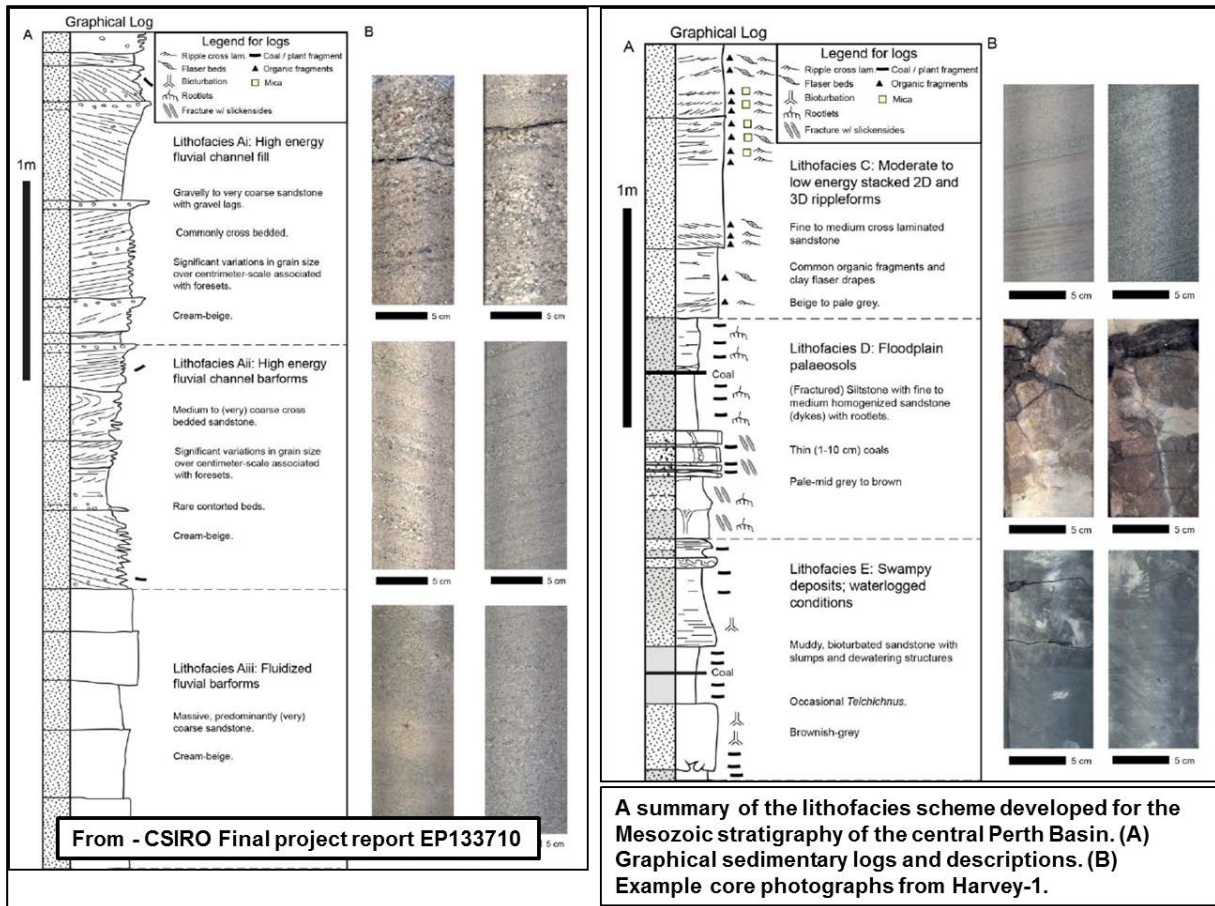


Figure 5.6: Example of core facies in Harvey-1 (Piane, et al., 2013)

The upper part of the **Yalgorup** is formed by mixed high energy sandstone (Ai to Aiii), moderate energy sandstones (B) and low energy ripple marked sandstone (C). A mudstone bed up to 2 m thick is also present intercalated with the sands. The middle and lower parts of this member consists mainly of siltstones and sandstones representing paleosols (D).

So, the Yalgorup consists of a rapidly-switching, on the order of 1m, mixed lithofacies, with the exception of extensive floodplain paleosols in the lower Yalgorup. However, even within this soil profile there is rapid switching in the sandstone dykes, between high

energy channel fill and moderate energy channel barforms, indicated by the variation in grain size.

The Wonnerup mainly consists of continuous high energy sandstone. (Ai to Aii) that may be occasionally punctuated by medium energy sandstone (B) or low energy ripple forms (C) and very rare punctuations of siltstone/mudstone beds. When they occur, they are mainly overbank type of deposits (G) and occasionally finely interbedded indicating crevasse-splay deposition (F) or swampy lagoonal environments (E). These appear in the lower part of the Wonnerup member.

The Wonnerup member is more homogeneous in terms of lithofacies development. However, within a lithofacies unit, there is still rapid-switching between crossbeds and foresets, indicated by 1-10cm beds of alternating grain-size sandstones. These are primarily high energy channel fill and barforms, with rare lower energy rippleforms and swampy/lagoonal deposits.

The Lesueur Sandstone contains over 60% of high energy channel fill and barforms (facies Ai-Aiii). Its two lithostratigraphic members, the Yalgorup and Wonnerup contain approximately 35% and 85% of facies Ai-Aiii, respectively.

6. RECOMMENDATIONS FOR PALEOSOL FACIES MODELLING.

There are two types of mechanism that act in the generation of a paleosol: autocyclic and allocyclic (Beerbower, 1961), (Fedorko, 2011). The first type of mechanism is inherent to the processes that take place in a particular sedimentary environment. For instance, in a fluvial system, the partial erosion of the paleosol by channelized bodies, variations on topography affecting the water-table depth, changes in the alluvial/fluvial system (channel avulsion), or differential erosion and/or compaction. Autocyclic pedogenic sequences are very difficult to correlate, as they are highly dependent on local basin factors and have reduced lateral continuity.

The allocyclic mechanisms however correspond to the operation of large scale controlling factors such as tectonic or climate regime. In contrast, allocyclic pedogenic sequences are much more continuous laterally and generally became good correlation markers.

For example, in 1993 Wright and Marriot, presented a model of pedogenic development in a fluvial system related to sea-level cycle, Figure 6.1. In this model low sea level periods (LST) produce strongly developed and well-drained paleosols cut by channel incisions whereas high sea level periods (TST) result in development of hydromorphic paleosols (waterlogged) with channel overlap due to initial low accommodation space. As the sea level rises and accommodation space increases rapid sediment accumulation takes place preventing soil development. In the final stage of high sea level (HST) low accommodation space is predominant in the fluvial basin allowing the development of soils again.

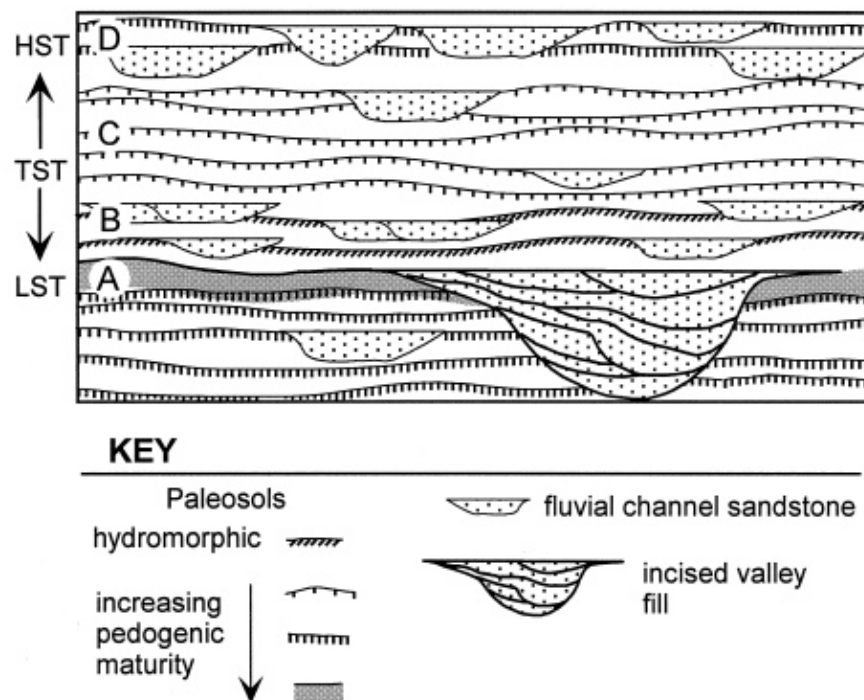


Figure 6.1: Pedogenic development in a fluvial system related to sea-level cycle (Wright & Marriot 1993 in (Kraus, 1999)).

According to modern analogues, soils are dependent on several of allocyclic factors that will condition their development, distribution and extend: Climate, vegetation, relief or topography and time.

Although soils are formed through autocyclic processes, in a fluvial system the thick accumulation of stacked paleosols horizons deposited over a long period of time (for instance, enough time to generate >500 m of section in Yalgorup), indicates that an allocyclic process must have been the main cause for this large development. The external allocyclic process affecting the Harvey area paleosols could have been a tectonic event or climate change that affected the entire basin.

In summary, the great thickness (~150m) of the paleosol dominated interval and the total thickness of the Yalgorup Member. (>500m), probably imply stability during a long period of time of the allocyclic factors that could have intervened in the paleosols development. Stable tectonic and climatic conditions in the Perth Basin during the Late Triassic would have potentially allowed extensive development of vertisols in the area. Large and irregular shaped paleosol bodies can be expected covering tens or even hundreds of Km².

Although allocyclic processes are probably the main cause for the development of such a thick paleosol interval in the Harvey area, autocyclic processes have still taken place and need to be taken into consideration. For instance, the partial erosion of paleosols by channelized bodies at certain times breaks up the paleosol continuity. Differential erosion and/or compaction, variations in topography affecting the water-table depth, or changes in the alluvial/fluvial system (channel avulsion) will affect the lateral continuity of the paleosol at a smaller scale. This facies variability has a direct impact on the petrophysical characteristics of the paleosol unit and needs to be captured in the model, as it will affect the K_v/K_h ratio, and the tortuosity of the plume migration pathways.

J M. Kraus, 1999 presents a diagram (Figure 6.2) showing the range of paleosols that can form in a thick vertical section depending on whether sediment accumulation was steady or discontinuous. This diagram shows three different cases corresponding to different sedimentation rates associated to different small-scale basin conditions. This conceptual section could easily represent the Yalgorup Member stratigraphic architecture.

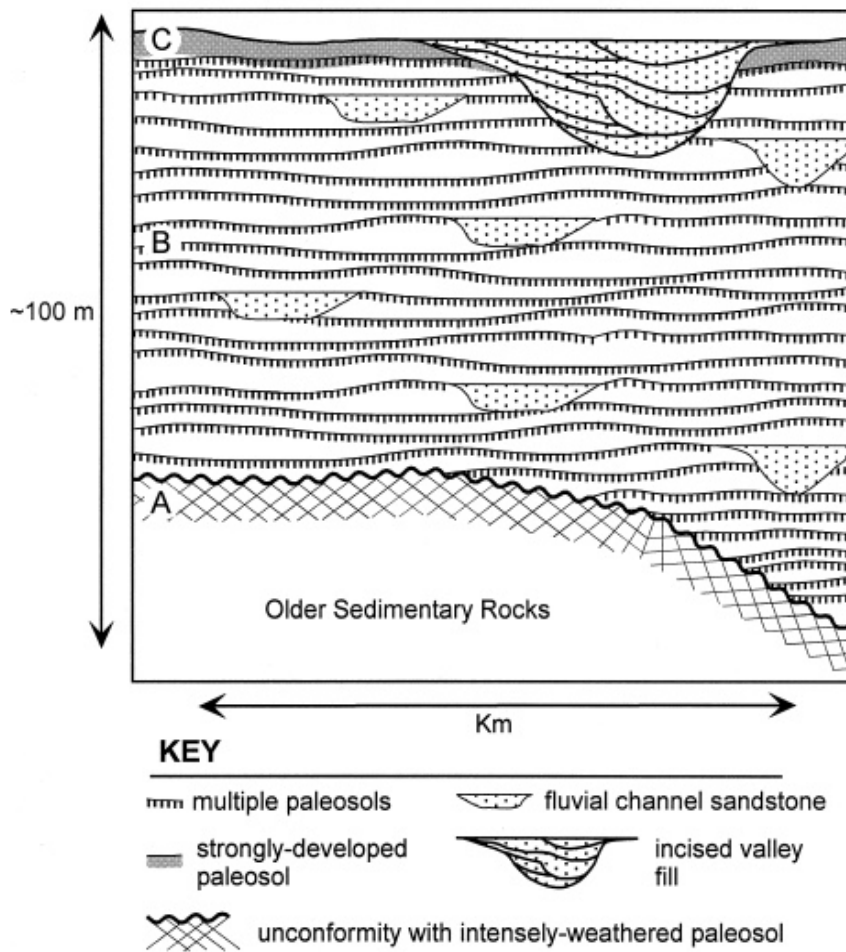


Figure 6.2: Different sedimentation rates associated to different small-scale basin conditions (Kraus, 1999).

The primarily terrestrial deposits of the Bowie and Wichita Groups on the north-eastern portion of the Eastern shelf constitute a good analogue for the paleosols of the Yalgorup Member. This series reach a thickness of up to 530m in the east of the basin and thin westward towards marine-dominated strata. Three terrestrial facies are recognized: (1) sand- and gravel-rich channel-bar facies; (2) point-bar facies; and (3) floodplain facies. Sand and gravel rich, channel-bar facies were deposited by braided stream systems fringing the north-eastern highlands, whereas the point-bar facies record meandering stream systems that developed on the Eastern shelf to the south and west of the braided stream system. These depositional environments are very similar to those recognised in the Harvey area.

Reconstruction of paleocatenas (e.g. fluvial channels and their associated floodplains) was limited to a few laterally continuous outcrops in the scale of hundreds of metres to 1-2 kilometres long. These references to fluvial plain paleosol dimensions could be useful to define the geometry of the Yalgorup/Eneabba paleosols complex. Although the lateral variability derived from outcrops in the Midland Basin is large, it can be assumed that for thicknesses in the scale of a few meters, the paleosols could extend for hundreds of meters to several kilometres.

Finally, another case study that has been used as an analogue for the Yalgorup paleosol interval is the Triassic Hawkesbury sandstone in the Sydney Basin (Rust, et al., 1986). In their paper, mudrock beds with a typical thickness of 1-2m are described. The most common facies in this mudrock beds are ripple-cross-laminated, fine sandstone to siltstone and horizontally laminated ("pin-stripe") fine sandstone to siltstone to shale. These facies are intergradational and represent relatively long-term sedimentation on a portion of the floodplain remote from active channels. Common abandoned channel fill intersecting the mudrock beds in some outcrops are also described.

These facies (which are similar to the Yalgorup paleosol facies), can sometimes reach larger thicknesses up to 9-12m (Standard, 1969) or even 35m (Herbert, et al., 1972), and extend laterally for 2.5km in a coastal outcrop near Sydney.

In conclusion, paleosol facies are by nature extensive and irregular in shape which have a small average thickness and present rather continuous petrophysical properties. Given enough time under stable climate and tectonic conditions these facies can develop to form thicker and more extensive packages over a basin. Although dimension rules for these bodies have not been defined, it seems fair to assume that they extend for many hundreds of meters. That is, paleosols are essentially extensive facies bodies.

The Yalgorup materials were deposited over a period of about 27 my reaching a total thickness over 500m. In the Perth Basin at the time of sedimentation of the Yalgorup/Eneabba paleosol complex there was tectonic stability dominated by thermal subsidence and a suitable warm temperate climate, alternating dry and wet periods, sustained during enough time to have allowed the development of extensive paleosol formations at basin scale.

Nevertheless, some variations within the paleosols are to be expected due to the autocyclic nature of paleosols developed in a fluvial plain. For instance, presence of intersecting abandoned channel fill or sand filled desiccation cracks. The average paleosol facies thickness observed on core data from GSWA Harvey 1 well, indicate that individual paleosol bodies are between 2.5 to 3m thick. From the literature explored during this phase of the project it can be assumed that series in the order of a few meters in the vertical scale can extend laterally for several hundreds of meters.

7. STATIC MODELLING

The input data used to generate the 3D model comprises the latest data reviews, interpretations and analysis results carried out by number of subsurface disciplines as part of this project. The location map below (Figure 7.1) outlines the various areas and key elements that will be referenced throughout this report.

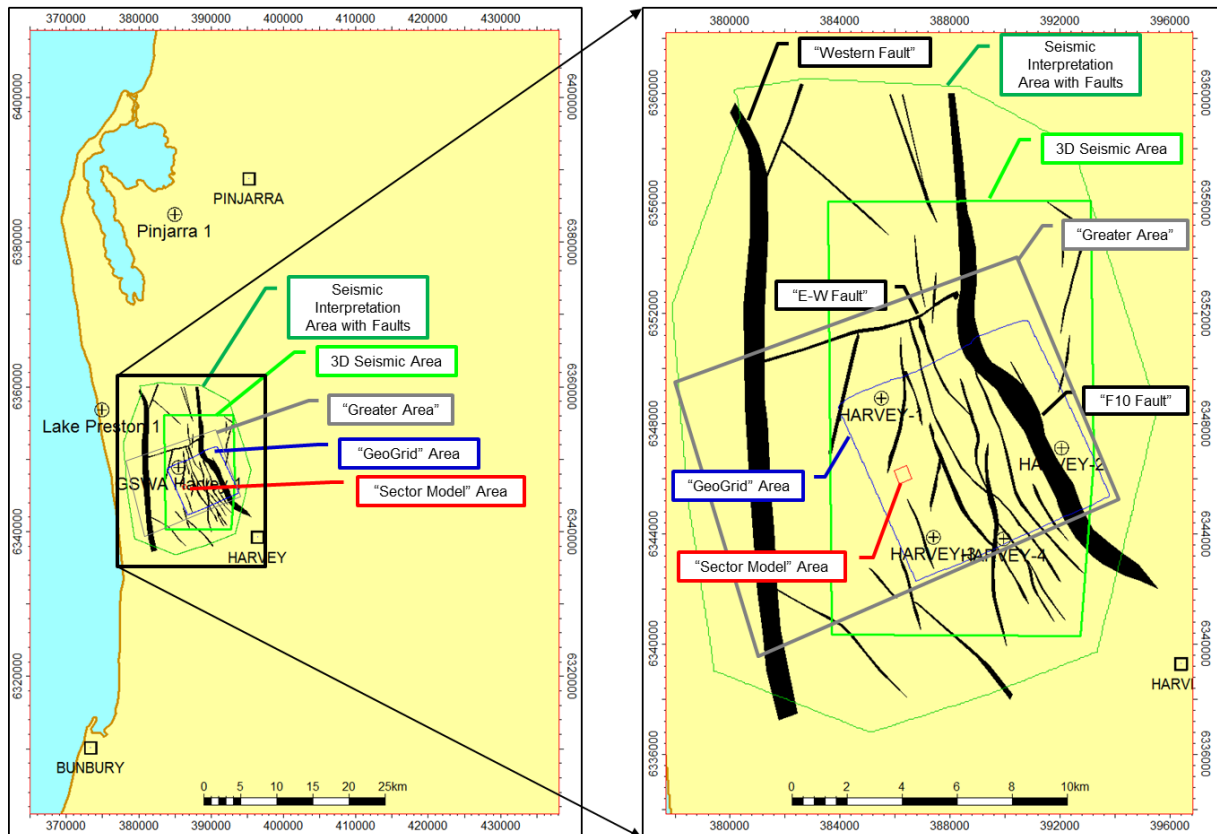


Figure 7.1: Location Map Showing Key Elements and Areas

7.1 Well data

There are four well penetrations with only one well drilling through all of the Wonnerup, the other three wells drilled between 100-223m into the Wonnerup. A reasonable coverage of wireline data is available for the four wells. There have been several cores acquired and analysed. There is also a 3D seismic survey over most of the study area with some 2D lines to cover the remaining area.

7.2 Geophysics and structural concept for the area

The results of the seismic interpretation constitute the structural and stratigraphic framework that have been used to generate the 3D static modelling grid. The data set used comprises a 2D and a 3D survey (Figure 7.2).

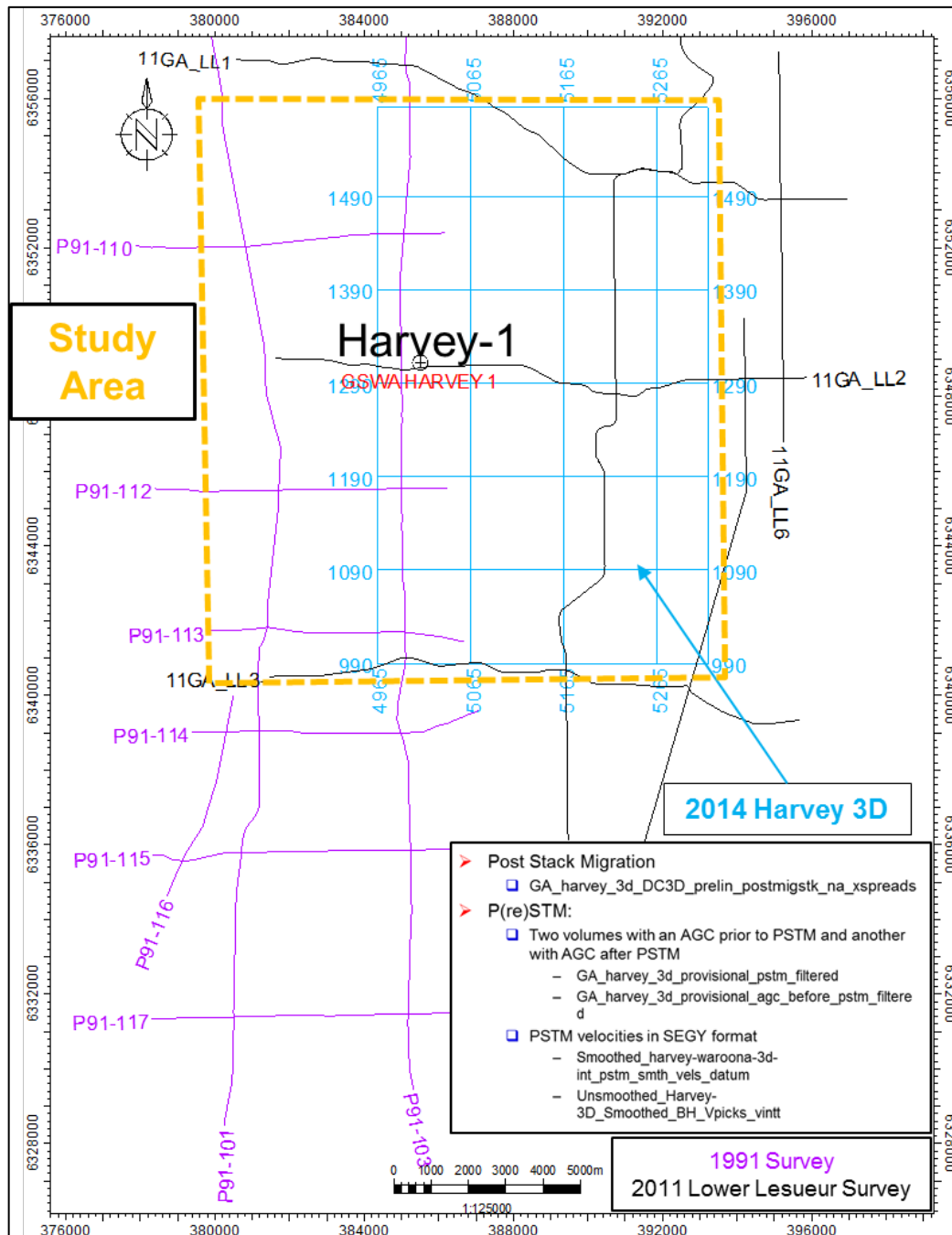


Figure 7.2: Seismic Survey Map

Reprocessing of the Harvey 3D seismic volume was undertaken by Curtin University has enhanced the data quality in comparison to the previous version done by Velseis in Brisbane. In particular, fault imaging has been improved as has the general signal to noise ratio in the data. However, due to limited access during data acquisition there are significant data gaps within the volume.

The 3D seismic dataset covers a total of 115km² but is poor in places due to access constraints (~40% of surface area) when acquiring the data (Figure 7.3). This has greatly influenced data quality below and adjacent to the multiple shallow data holes and its impact is particularly pronounced in the north-western part of the 3D and patchy shallow quality below and adjacent to the multiple shallow data holes. The data quality over the deeper primary zones of interest (i.e.: Yalgorup member, Wonnerup member and fault locations) ranges from poor to good (Figure 7.3).

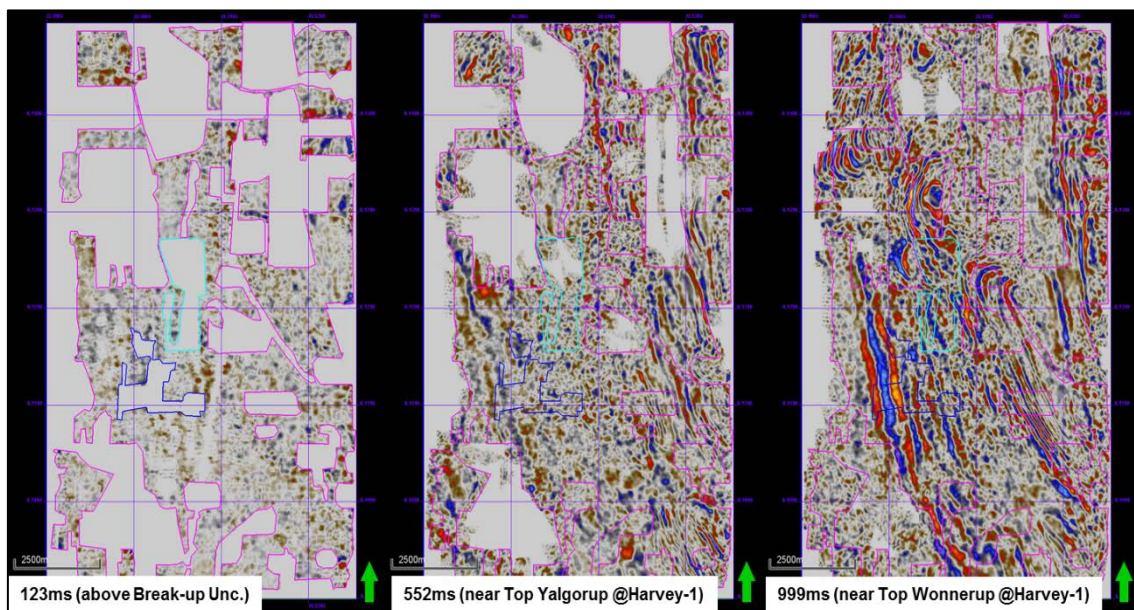


Figure 7.3: Shows Gaps in Seismic due to acquisition constraints

A detailed interpretation of horizons and faults has been completed. Additional horizons within the Yalgorup Member and the Wonnerup Member have been included compared to the previous study. The fault interpretation comprises greater detail as the reprocessing has provided a clearer seismic image.

In general, there appears to be defined by two sets of fault orientations. The area is dominated by a north-northwest-south-southeast trending fault (“F10” fault). In the downthrown section of the main fault, there are a series of en-echelon sub-parallel faults with two distinct orientations, these are north-south and north-northwest and south-southeast. (Figure 7.4).

The fault orientations on the map are consistent with those indicated in the Rose Plot displays for GSWA Harvey-1 and DMP Harvey-4. The magenta dashed lines on the map at (Figure 7.4) are representative of the fault trends near DMP Harvey-4, these are very similar to the two trends indicated in the Rose diagram. The Rose diagram for GSWA Harvey 1 shows a single dominant trend of north-northwest to south-southeast, which is consistent with the orientations of the faults in the area.

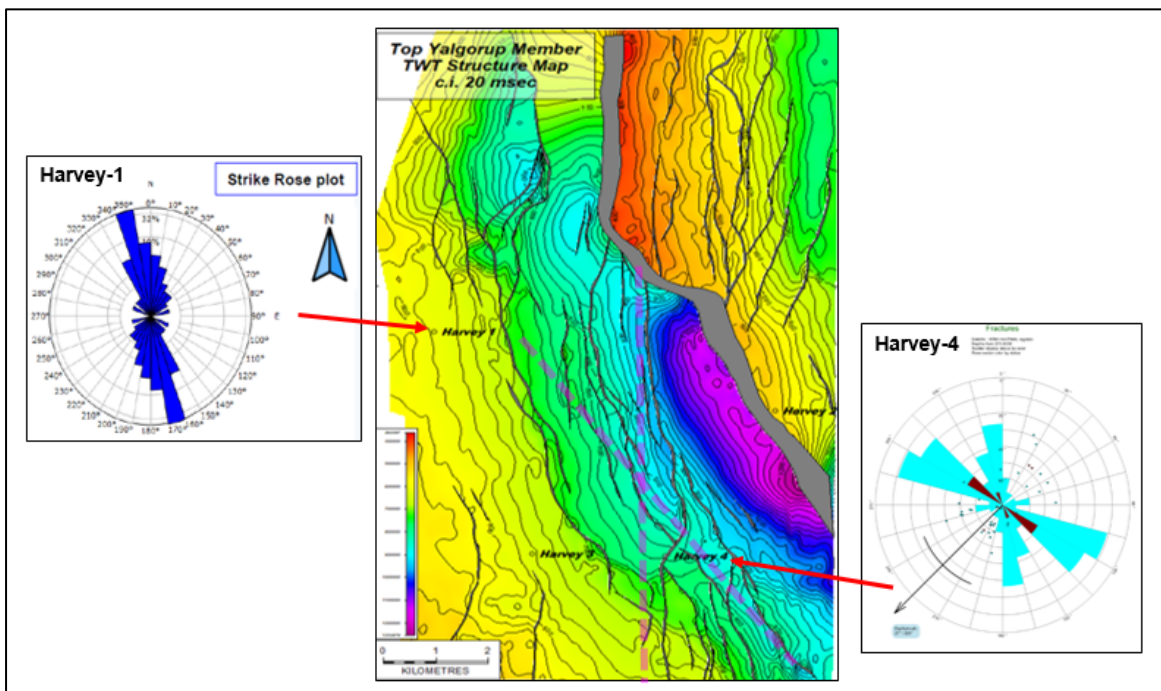


Figure 7.4: Fault orientations

Six horizons were interpreted across the Harvey 3D area. These are listed below and shown in Figure 7.5;

1. Top Yalgorup Member
2. Intra-Yalgorup Marker
3. Top Wonnerup Member
4. Intra Wonnerup Marker 2

- 5. Intra Wonnerup Marker 1
- 6. Top Sabina Sandstone

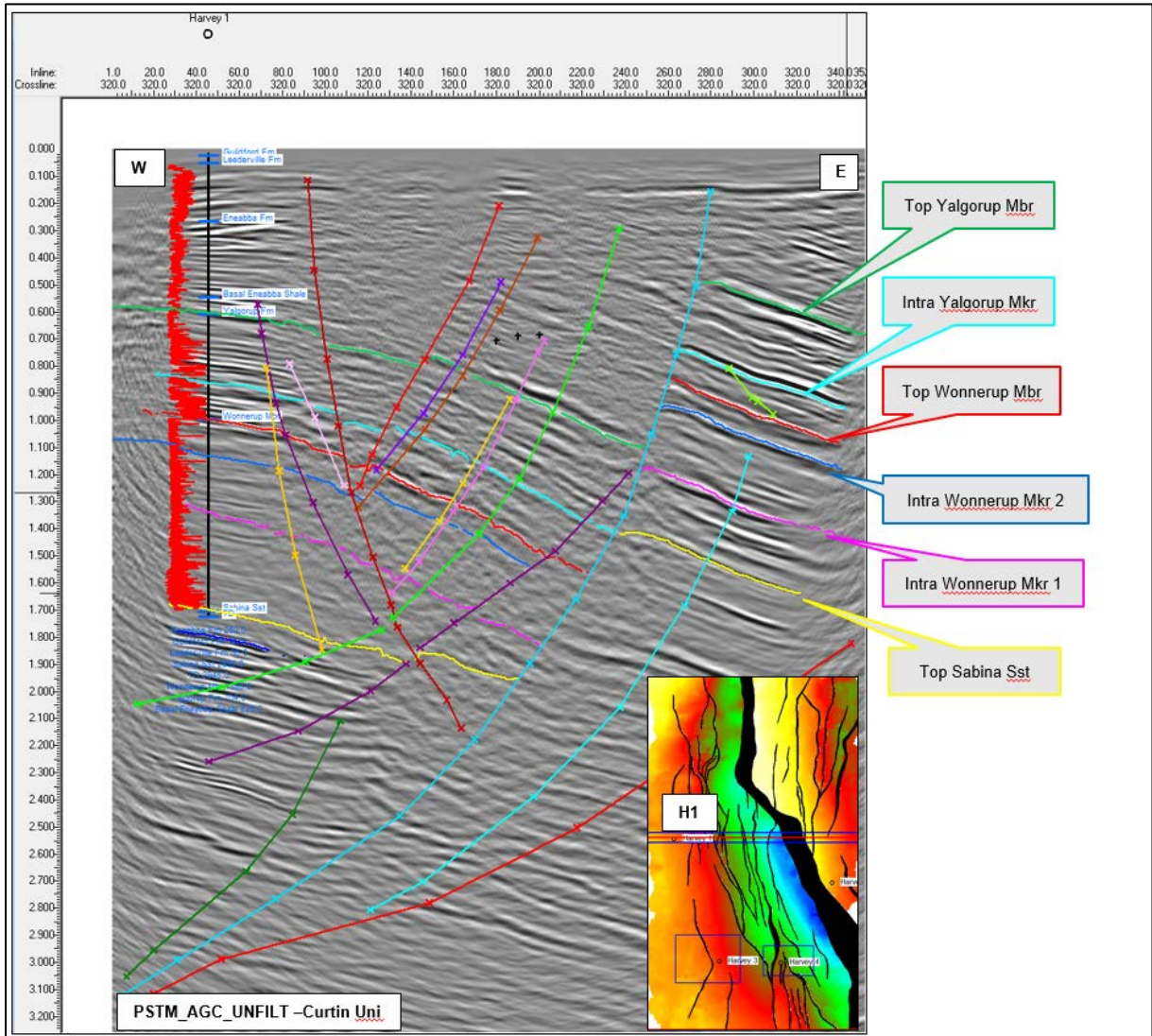


Figure 7.5: Horizons interpreted with GSWA Harvey 1 well tie

Given the straight forward nature of the velocities across the study region, conversion of the two way time surfaces to depth was simply achieved by multiplying the two way time grid (correcting for two way time) by the average velocity grid. Finally, to correct for any residual errors (which is usual), the resultant depth grid was re-gridded to tie the well tops for each surface yielding the final, well-tied depth surfaces for each of the mapped surfaces. The final depth maps are provided below (Figure 7.6 to Figure 7.11).

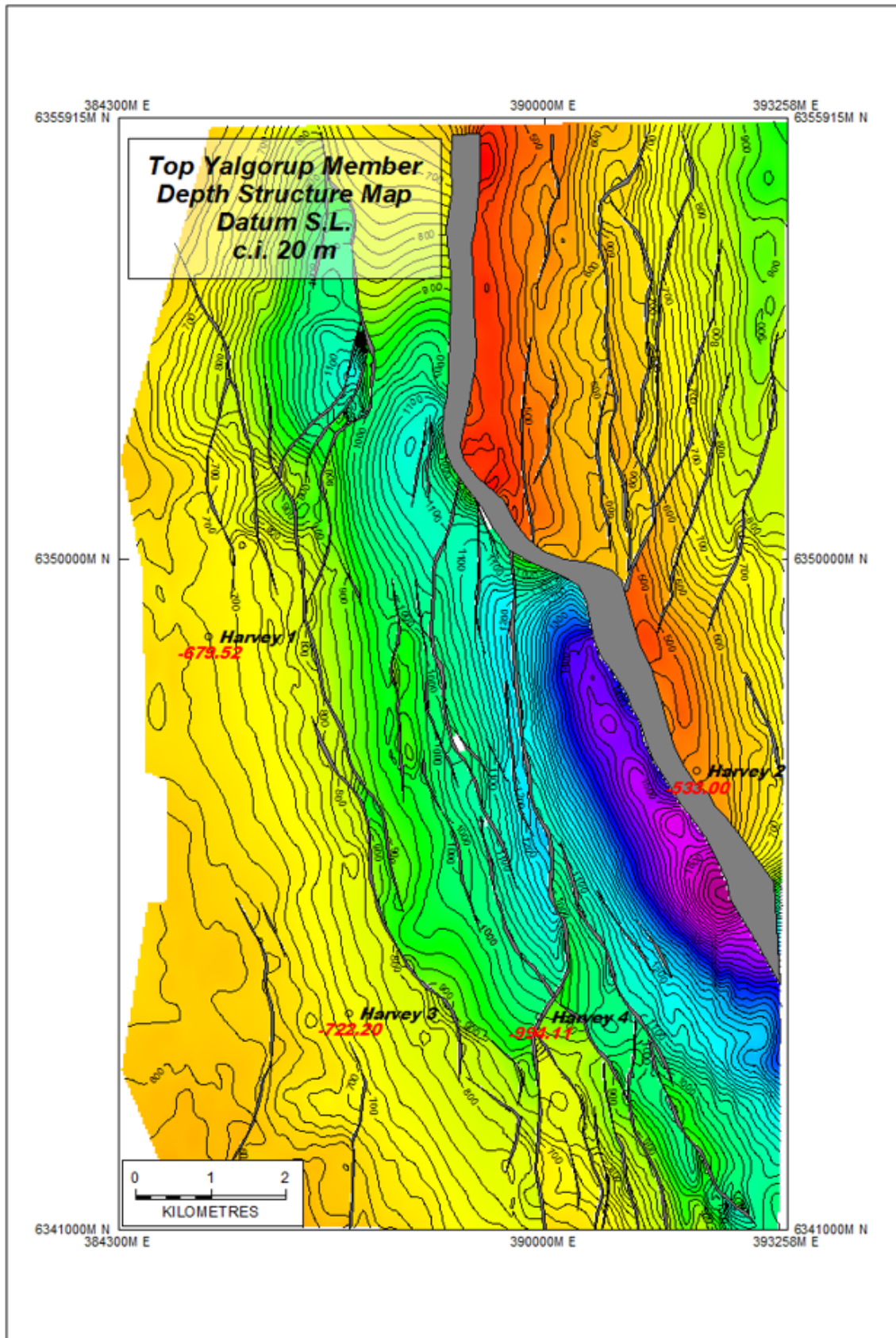


Figure 7.6: Top Yalgorup Member Depth Map

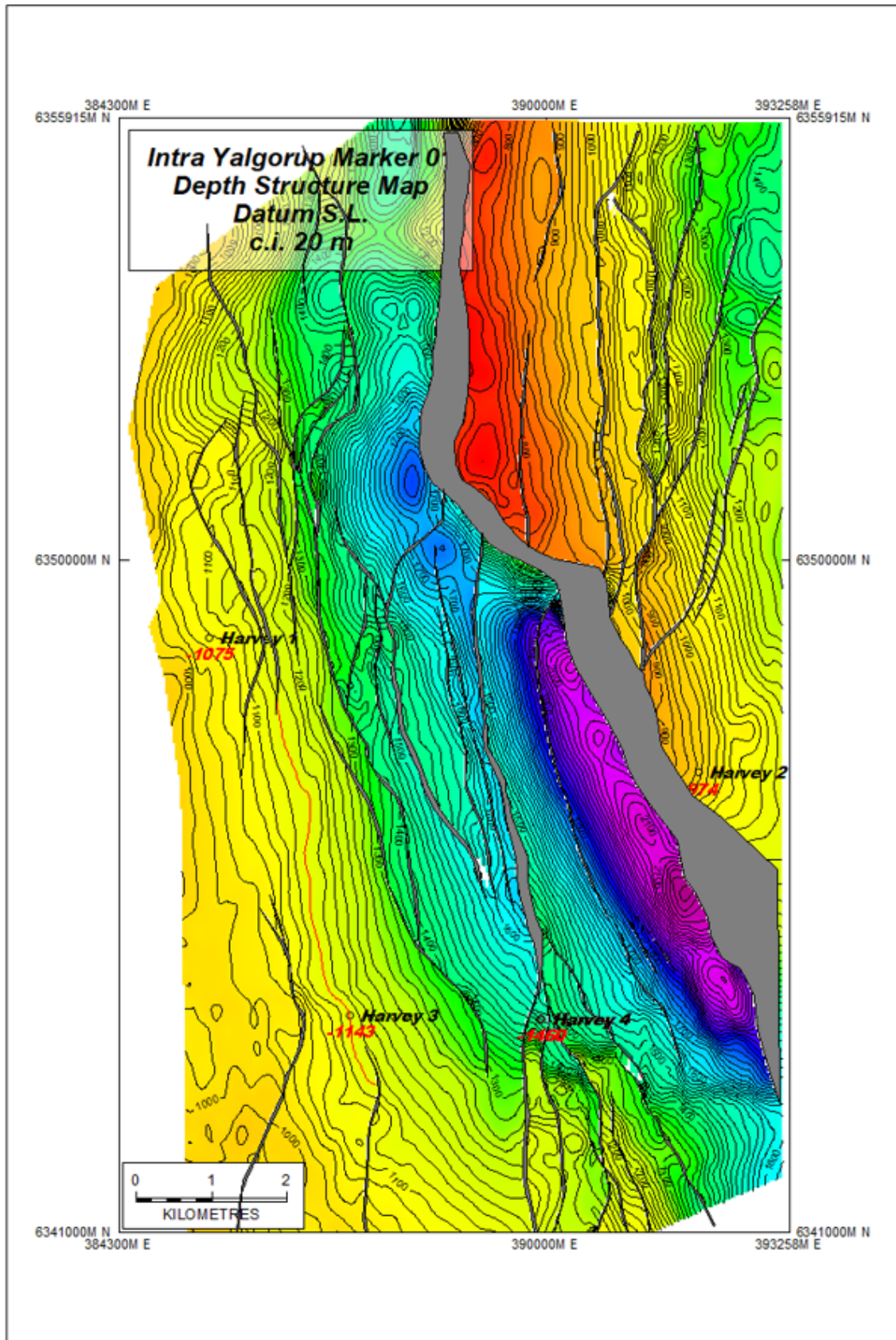


Figure 7.7: Intra Yalgorup Marker 01 Depth Map

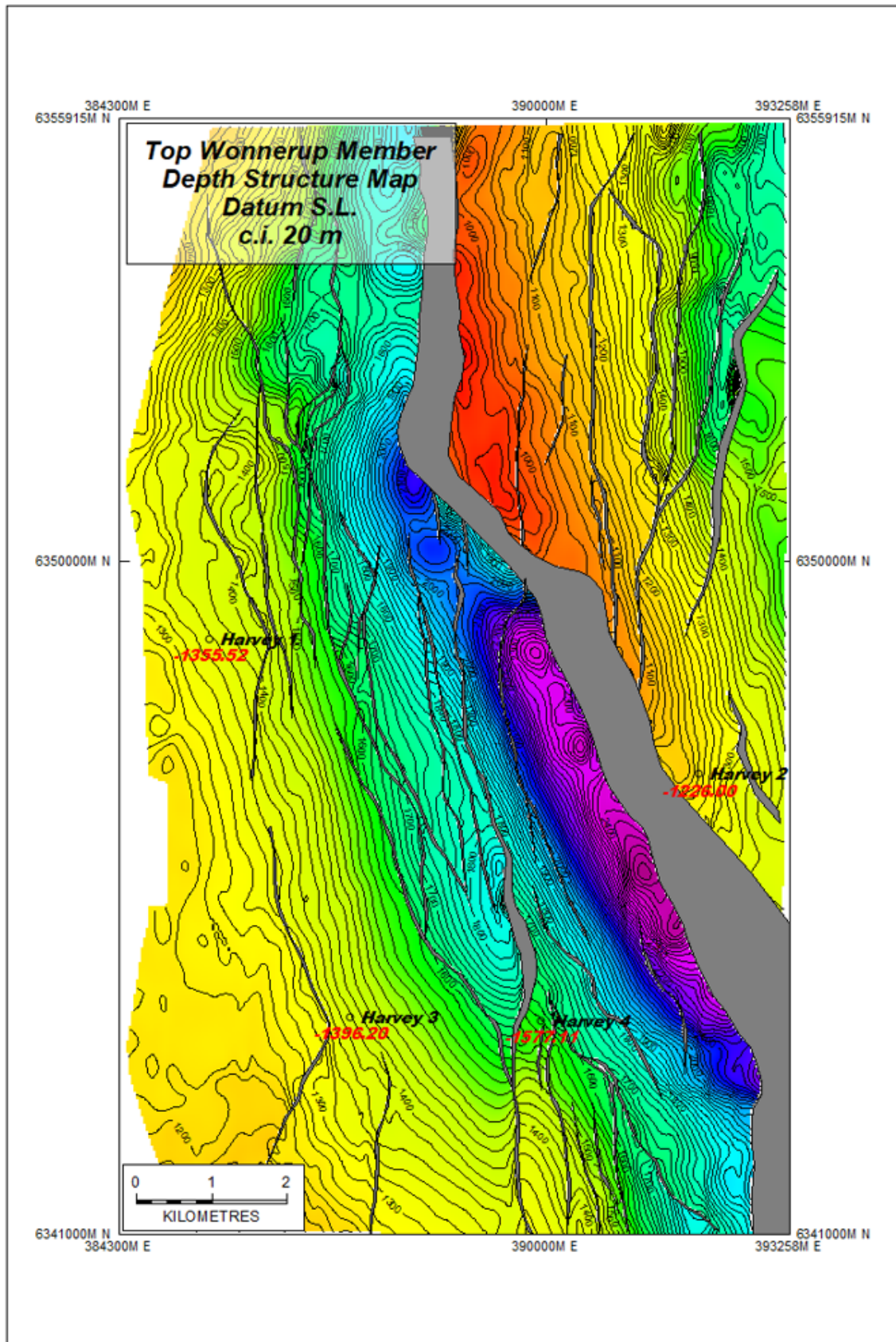


Figure 7.8: Top Wonnerup Member Depth Map

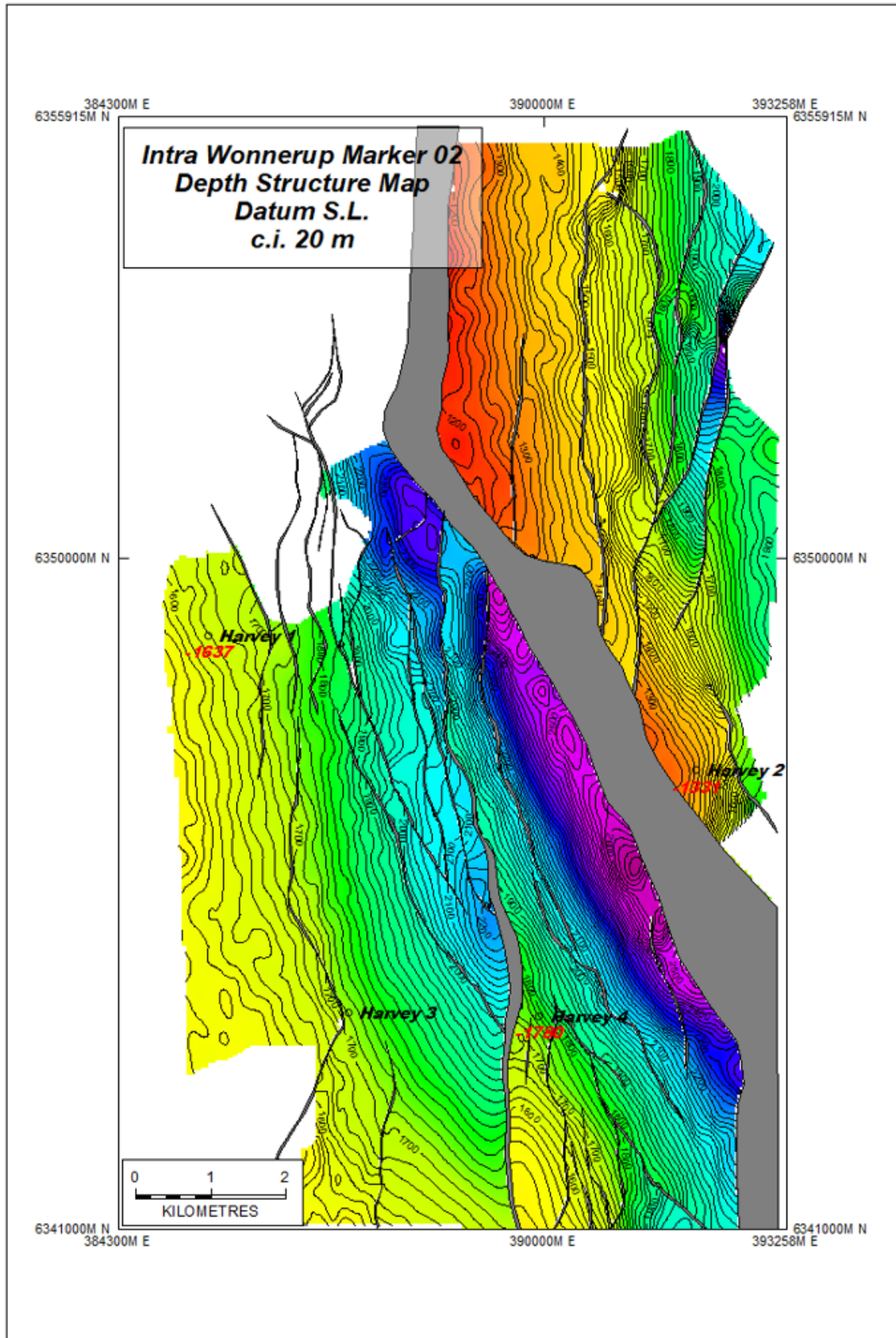


Figure 7.9: Intra Wonnerup Marker 02 Depth Map

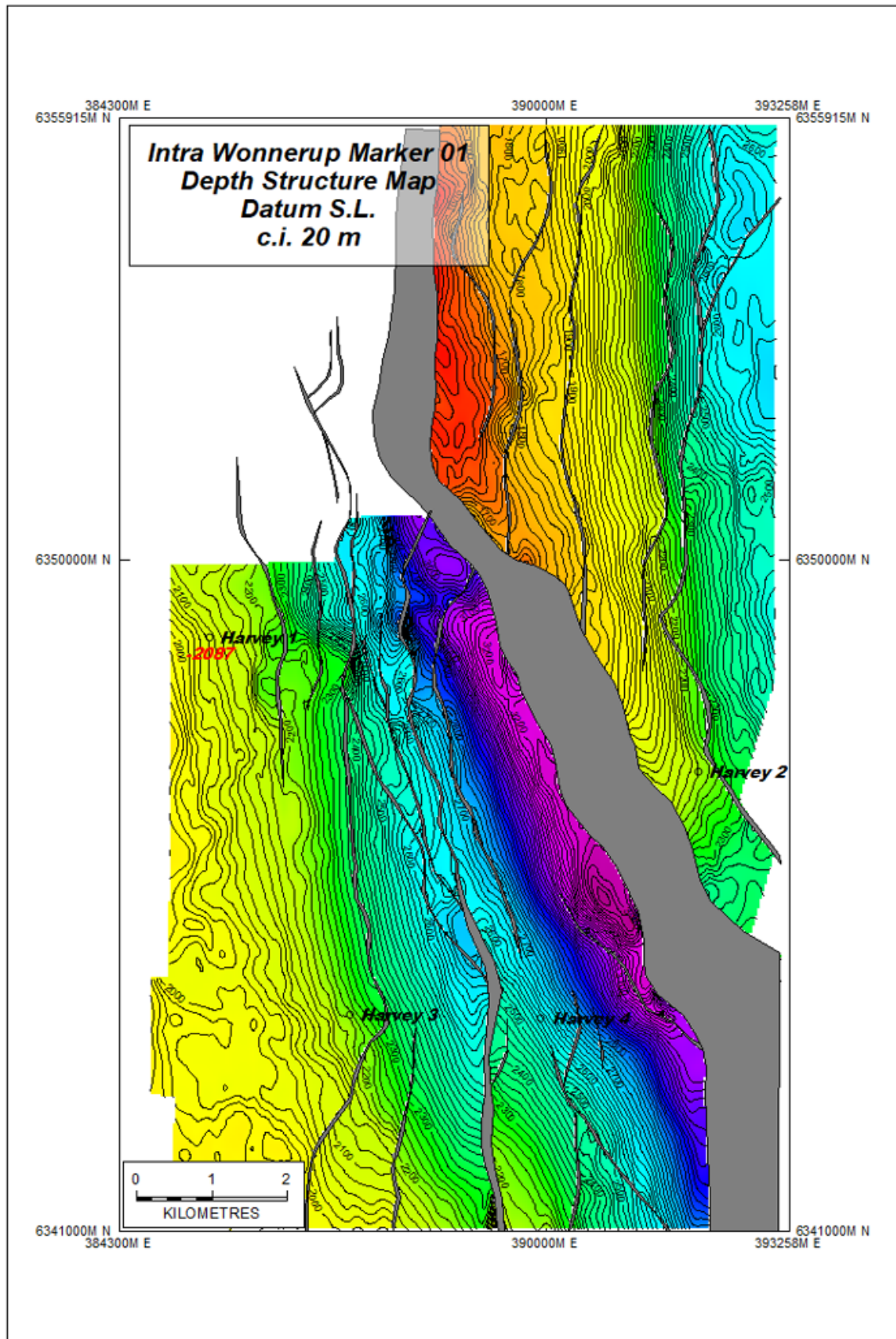


Figure 7.10: Intra Wonnerup Marker 01 Depth Map

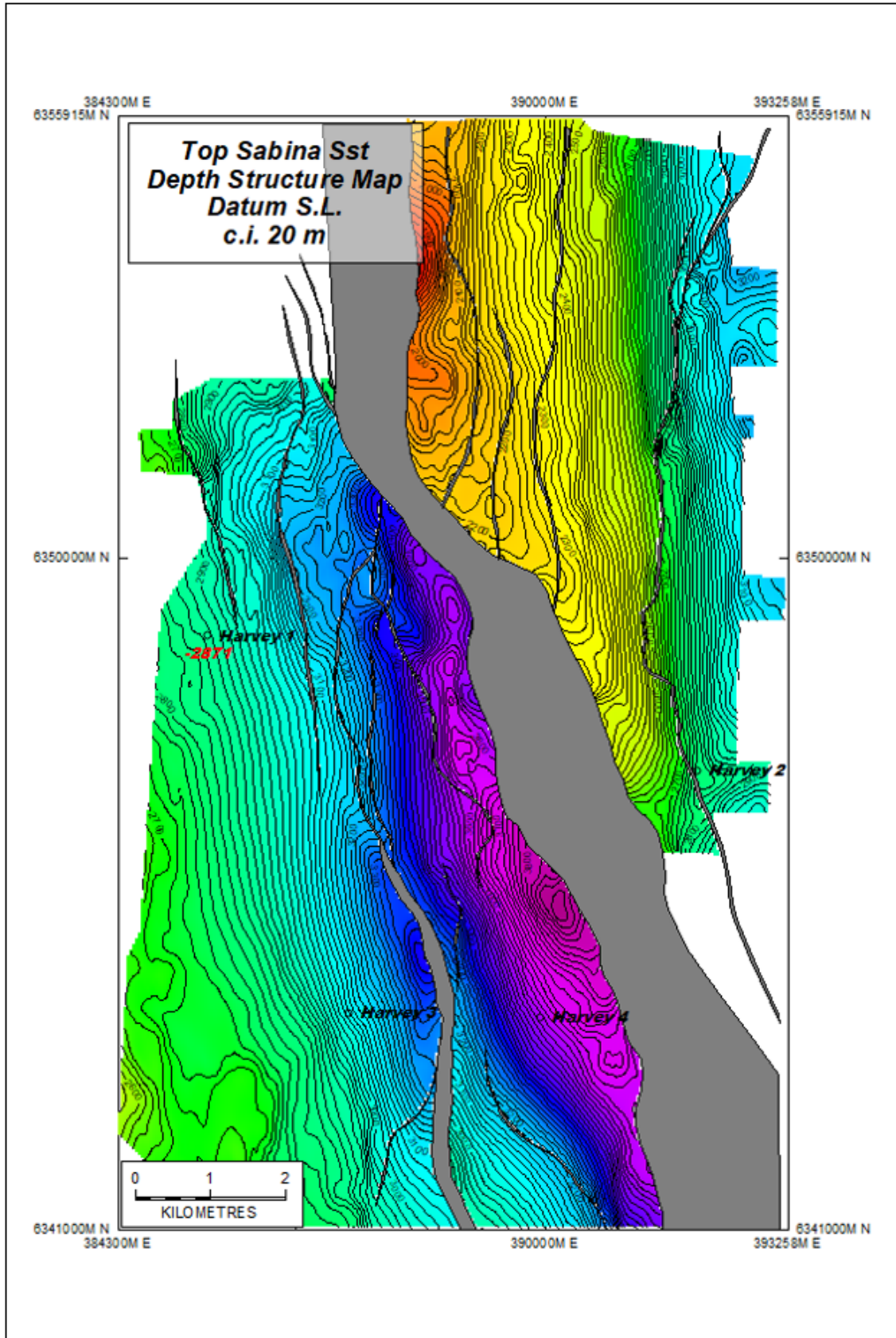


Figure 7.11: Top Sabina Sandstone Depth Map

7.3 Well correlation

A regional correlation based on twelve wells drilled over the southern Perth Basin has been the basis for the correlations of the four Harvey wells that will be the main control points during the 3D static modelling process.

This correlation has been mainly based on wireline data such as gamma ray log (GR), see Figure 7.12. Due to the non-marine nature of the deposits there is a lack of paleontological control for the Triassic-Jurassic section in this zone that results in an uncertain correlation in some areas.

In addition, the lack of associated acoustic logs and insufficient palynological data has also resulted in many difficulties to differentiate stratigraphic units in some wells, particularly in separating the Eneabba Formation from the underlying Yalgorup member of the Lesueur Sandstone.

Also, the fluvial depositional environment is extremely difficult to correlate locally from well to well, particularly the individual sands and as we do not expect them to be extensive enough to be penetrated by more than one well. There is more confidence of correlating packages, however, due to the number of possible outcomes these markers have not been used to divide the model into sub-zones.

The seismic has been used to assist with the correlation which does help with a mid-Yalgorup marker, but it was not very useful in the Wonnerup due to only one well penetrating the Intra-Wonnerup markers. Although there is uncertainty surrounding the geometry of the Wonnerup and Yalgorup members due to the large distance between the two type sections that define them, this has been accepted as a conformable stratigraphic relationship. Likewise, the Eneabba Formation appears conformably overlaying both members of the Lesueur Sandstone. The most consistent correlatable marker is the Top Wonnerup, which is characterised by a sharp decrease of the GR. This is the best seismic event mapped.

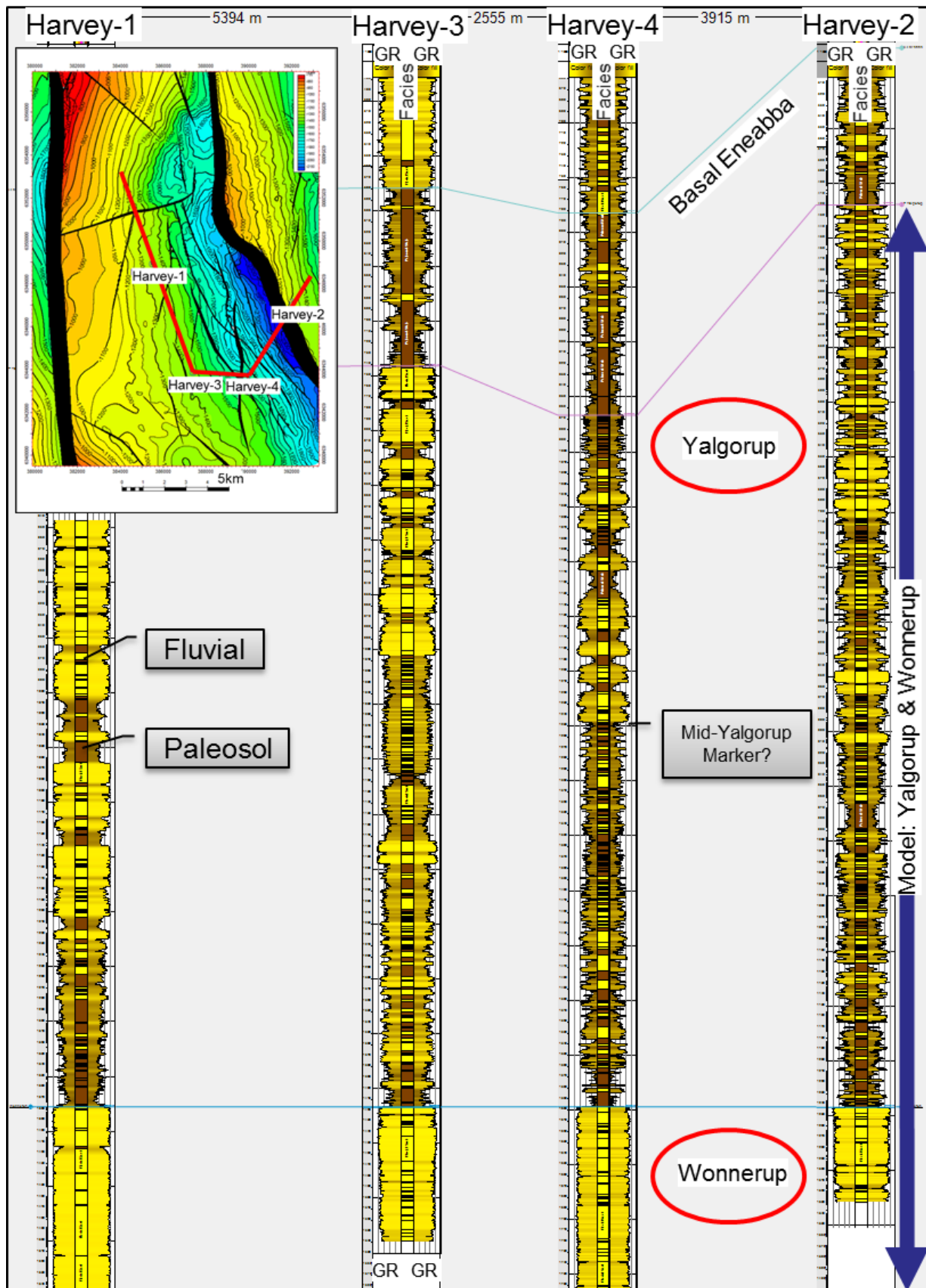


Figure 7.12: Correlation Panel

7.4 Petrophysical analysis

The log interpretation confirms the Lesueur Sandstone consists of interbedded sands and paleosols (Kennedy, 2015). The porosities of the sands in the Yalgorup member are of the order of 25-30% and in the Wonnerup they fall from 25% near the top of the member to 20% at TD in Harvey-4 (1740m). However, in Harvey-1 porosities fall to as low as 10% at the base of the Wonnerup (2840m).

In summary, good reservoir properties are recorded in the homogeneous Wonnerup member (1380-2895m depth). In contrast, the overlying Yalgorup (704-1380m) is far more heterogeneous with excellent porosities noted in the sand intervals. Full details are available in the ODIN report by Martin Kennedy – DMP/2015/3 (Kennedy, 2015) and the ODIN report by Mike Walker – DMP/2018/2 (Walker, 2017) with a brief summary below.

7.4.1 Review of current log Analysis

The original petrophysical analysis undertaken on the four (4) Harvey wells was reviewed (Walker, 2017). The interpretations carried out during previous analysis are adequate given the data acquired, porosity was well characterised. However, the permeability transforms needed revision.

7.4.2 Gamma ray response

Core gamma measurements were compared to the interpreted facies scheme. High to moderate energy, clean, channel fill and barforms (facies Ai to B) typically exhibit the lowest gamma response; facies C to D are intermediate, and facies E to G have higher gamma response.

However, there are overlaps in the gamma response from different facies types: The probability of **facies Ai-Aiii** is more likely to occur at gamma ray values between 10-50 counts per second. Facies B to D typically have intermediate values between 50 and 90 counts per second. For facies E to G, gamma ray values are most commonly in the range of 70 to 90 counts per second.

Using gamma ray alone to infer lithofacies types in non-cored intervals leads to a reasonable ‘rule-of-thumb’, but not a unique interpretation. A GR cutoff of 80 gApi to discriminate between sands and paleosols was used as a guide but manual picking and interpretation of the facies types was undertaken in this project.

7.4.3 Shale volume

Total shale thickness for the Yalgorup member is about 145m, based on a shale cutoff value of 50%. This thickness of shale is about 21% of the total thickness of the Yalgorup member, which is about 676m. However, for the Wonnerup member, with a total thickness of 1501m, the shale thickness is approximately 25m, less than 2% of the total thickness of this member.

7.4.4 Porosity

Neutron, density and sonic log data were used to estimate total, effective and secondary porosities. Secondary porosity is calculated from the difference between neutron-density porosity and sonic porosity. Secondary porosity that may result from feldspar dissolution and other lithic grains, increases with increasing depth from near to zero to about 8%.

A comparison between core and log porosity shows an acceptable match. The best correlation is between the effective density porosity and core porosity with a coefficient of determination of about 72%.

7.4.5 Revised Permeability

The same mathematical approach was used for deriving permeability as it was in the previous study (Kennedy, 2015), this being a second order polynomial.

$$K = 10^{**} (A + B\phi + C\phi^2)$$

Log derived total porosity was plotted against the NMR derived permeability

Figure 7.13 and Figure 7.14 show data from GSWA Harvey 1 and DMP Harvey 4. Figure 7.15 shows the NMR data from the Yalgorup member from DMP Harvey 4. Figure 7.16 shows the core data.

Drawing polygons around the core of the data allow the extraction of the following polynomials, which is an improvement on the previous transforms.

$K = 10^{(32.8 * \phi - 51.1 * \phi^2 - 1.9)}$ was derived for the Wonnerup

$K = 10^{(12.8 * \phi + 30.8 * \phi^2 - 3.2)}$ was derived for the Yalgorup

This new transform as resulted in a reduced permeability compared to the permeability derived for the Gen3 modelling.

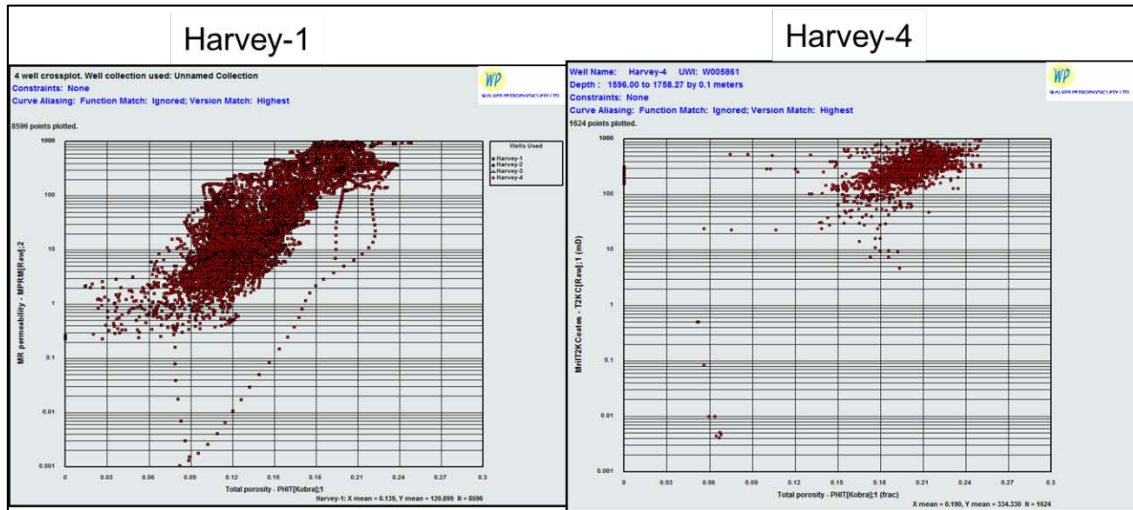


Figure 7.13: Wonnerup Log Derived Total Porosity vs NMR Perm

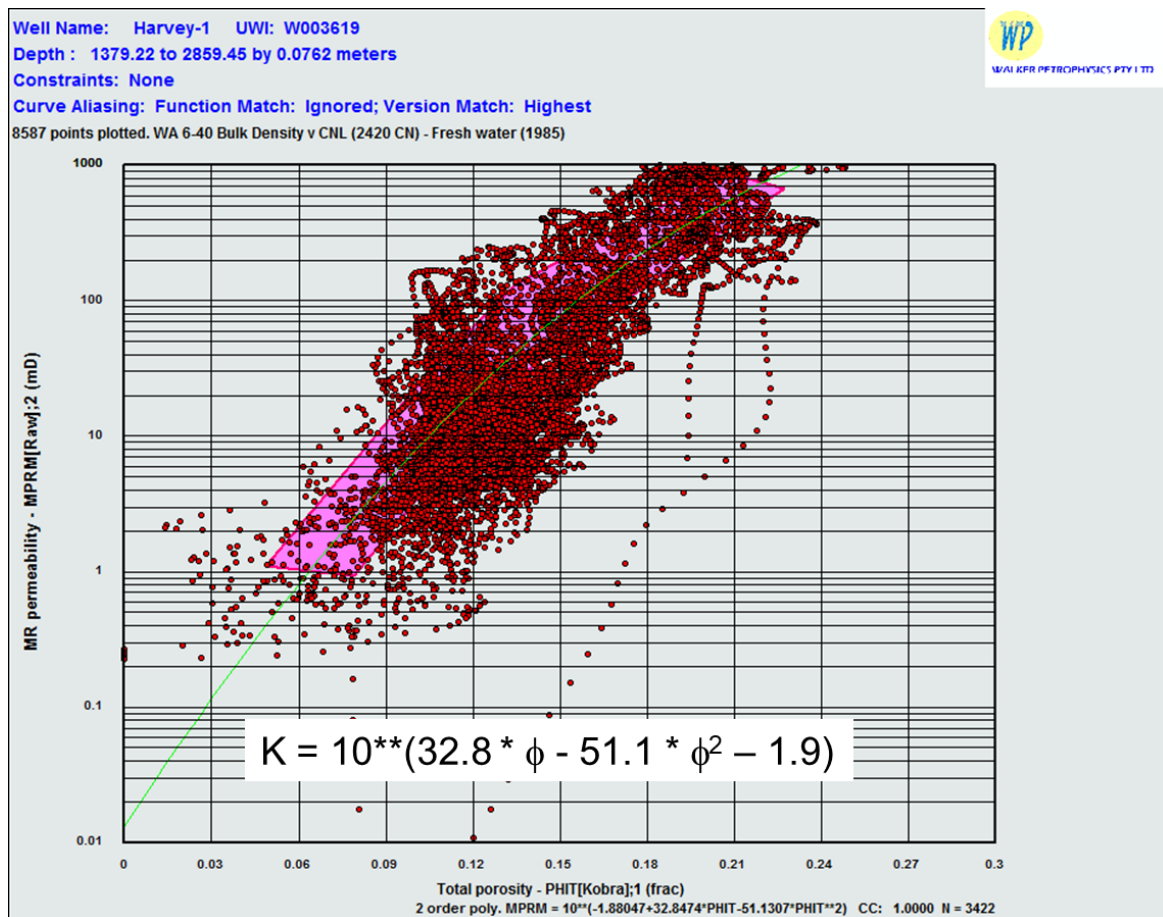


Figure 7.14: Revised Porosity Permeability Transform for Wonnerup

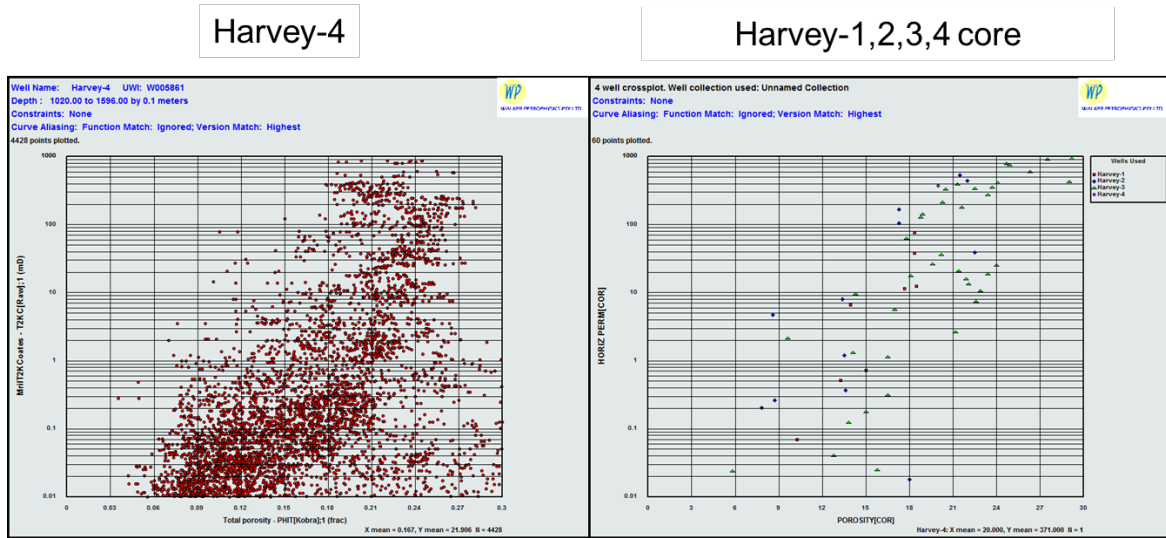


Figure 7.15: Yalgorup Porosity vs Permeability NMR (Left) & Core (Right)

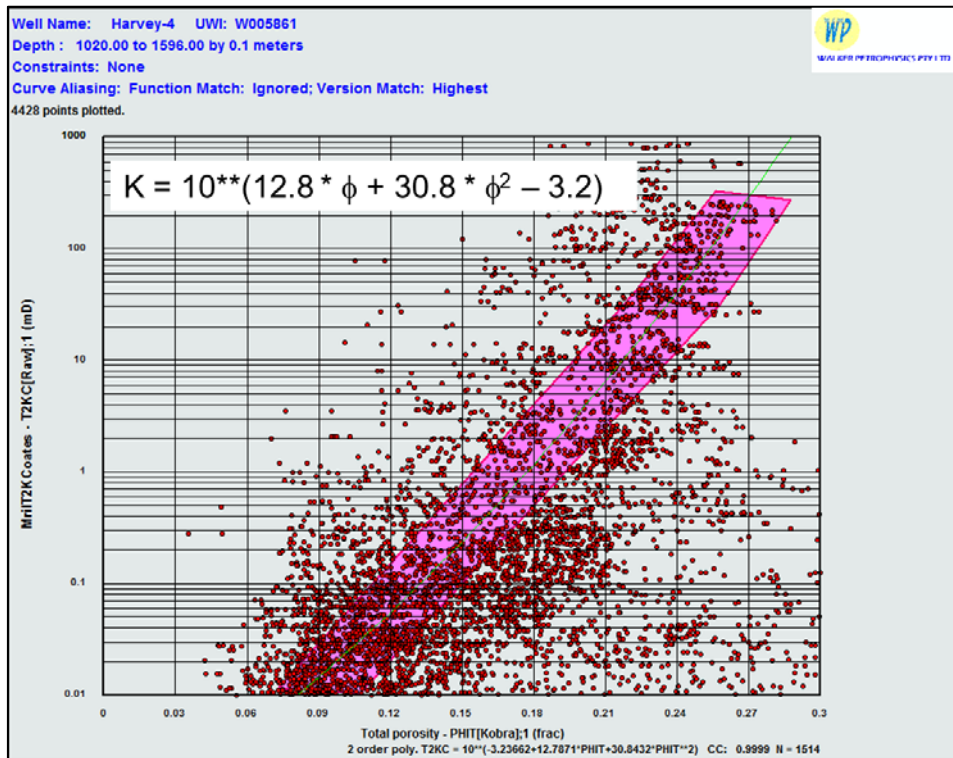


Figure 7.16: Yalgorup Porosity Permeability Transform

7.4.6 Sand/Shale distribution

GSWA Harvey 1 penetrated a thick sand interval with high net-to-gross (NTG) in the Wonnerup. However, there is only one well penetrating the entire Wonnerup section. The seismic shows very little reflectivity in the area which confirms to the results of the

well, but seismic reflectors are more pronounced away from the GSWA Harvey-1 well indicating a change in reservoir properties. As the NTG and sand shale distribution will control the Kv/Kh ratio and tortuosity of the pathway during CO₂ migration. It was prudent to adjust the “Reference Case” to reflect a lower NTG than what was interested at GSWA Harvey 1.

Therefore the “Reference Case” for this generation of modelling contained more heterogeneity than observed at GSWA Harvey-1 but a “Homogeneous Case” was still retained as a sensitivity.

7.5 Static modelling software

Static modelling was carried out using Emerson’s RMS software package. RMS was selected for this phase of modelling due to the number and complexity of faults interpreted. RMS also has the advantage of being able to vary the grid cell size away from the main area using ‘Control Lines’. This enables a finer grid around the injectors and coarser grid can be built away from the wells, therefore reducing the number of cells to be simulated.

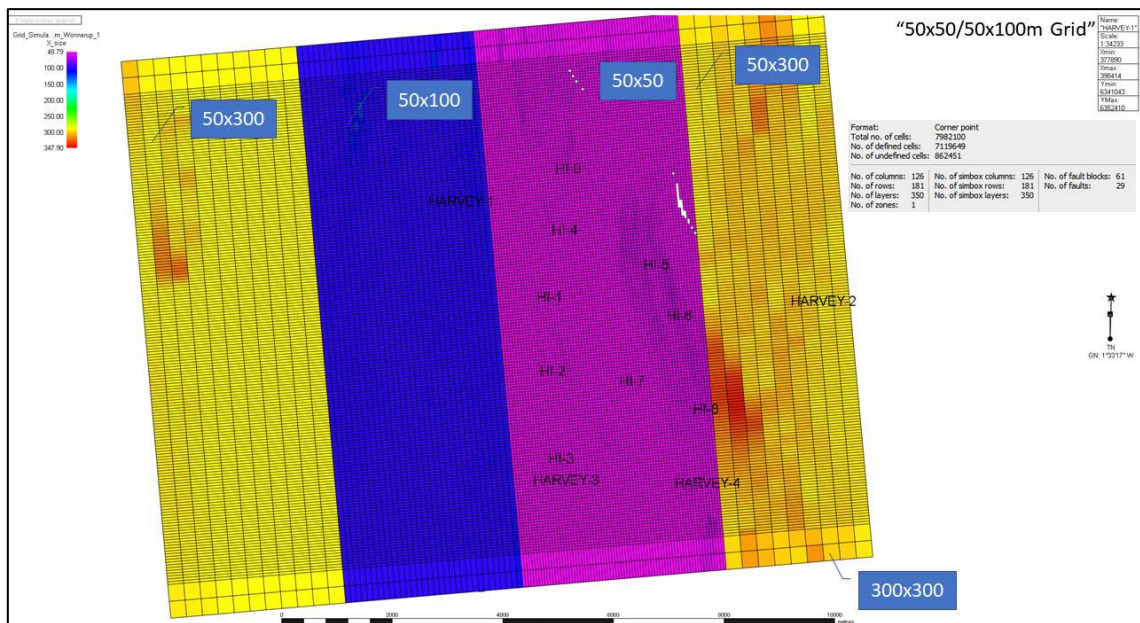


Figure 7.17: Example of grid dimensions using 'Control Lines' in RMS.

Depths were referenced to AHD (Australian Height Datum) across the area. The RMS project containing the input data and key models have been made available.

7.6 Data base

The RMS database has been loaded with all the available depth structure maps for the area with fault sticks and fault polygons. All of the wireline and petrophysical interpretation logs have been loaded.

7.7 Structural modelling

The fault model was built from the top Yalgorup Member to the base of the Wonnerup Member using the integrated structural framework method. The resulting 3D grid was smooth with no twisted or negative cells. An illustration of the input fault surfaces is shown in Figure 7.18.

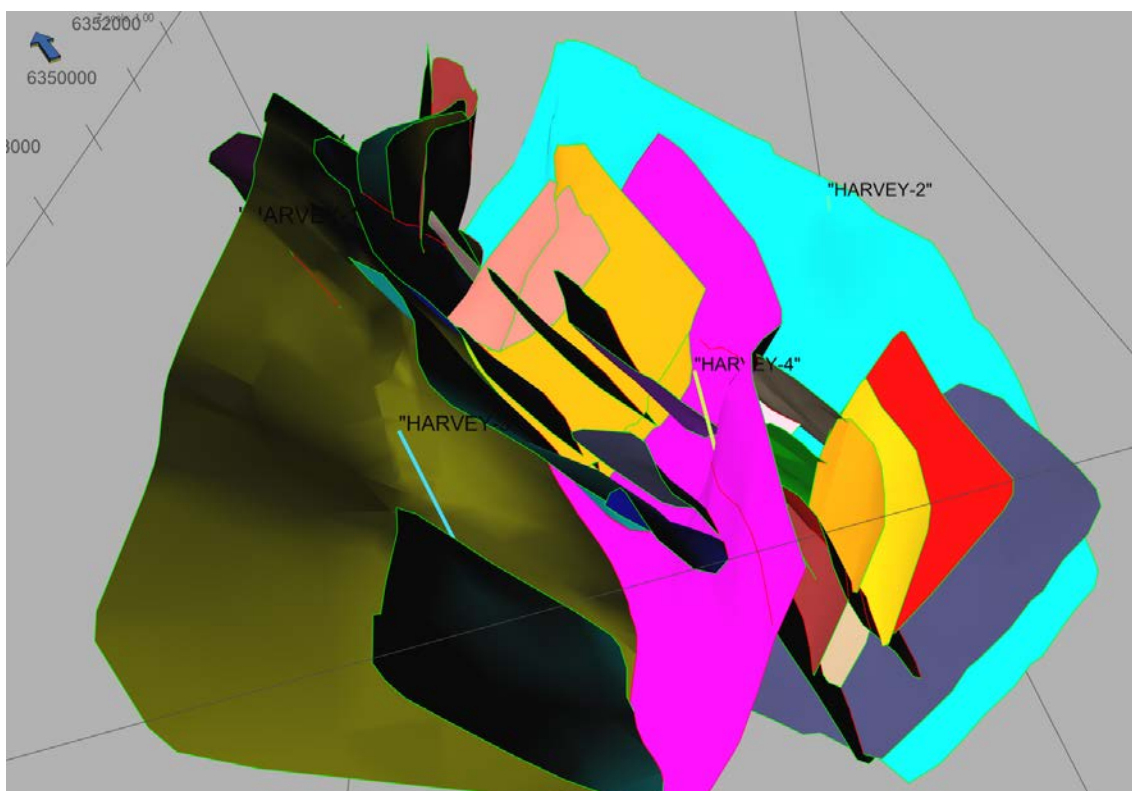


Figure 7.18: 3D View of Fault Surfaces.

The fault surfaces were edited and cleaned up prior to being used in the structural framework process. The resultant fault framework was then used to build the structural model via “Horizon modelling” from the top of the Yalgorup to the base of the Wonnerup members (Figure 7.19).

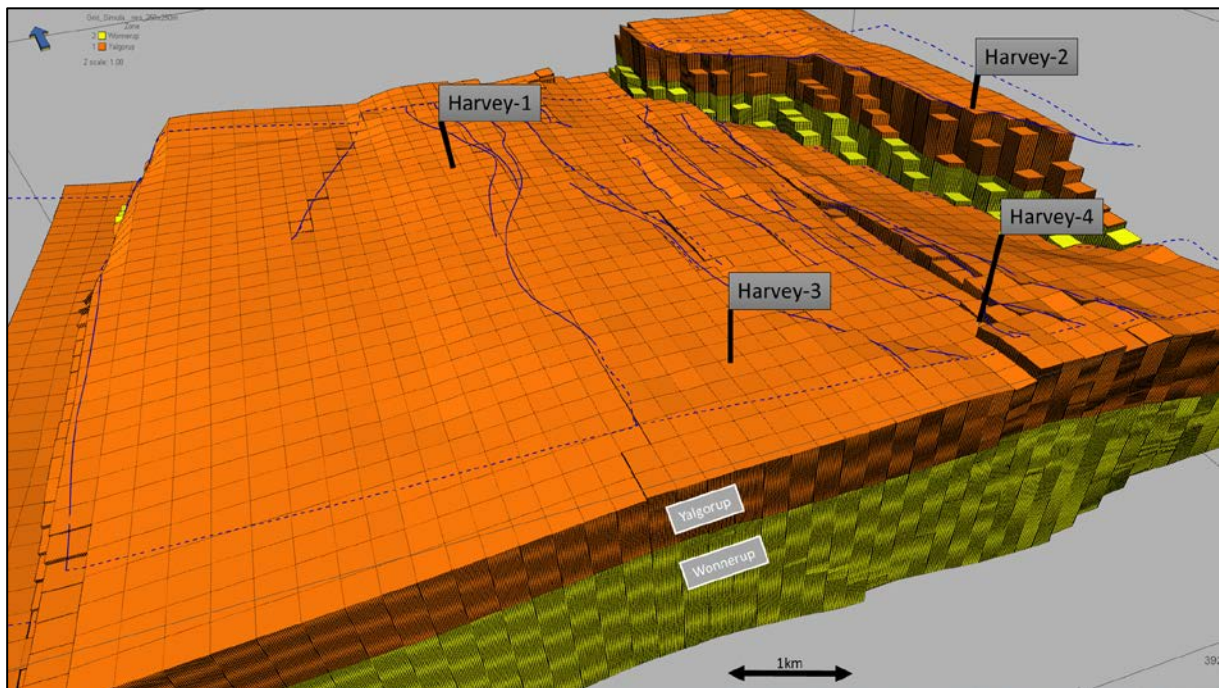


Figure 7.19: Structural Model with Faults

7.8 3D gridding

The two main zones (Yalgorup and Wonnerup Members) have been incorporated in the model. There were a number of grids created to find the balance between maintaining the detail required to predict plume movement within a limited number of cells that can be simulated in a reasonable timeframe. Grids at 25X25m, 50X50m, 100X100m and 250X250m were exported for comparison within the simulator. Details of the scenarios and upscaling results are available in the ODIN report by Lim, D., - DMP/2018/7.

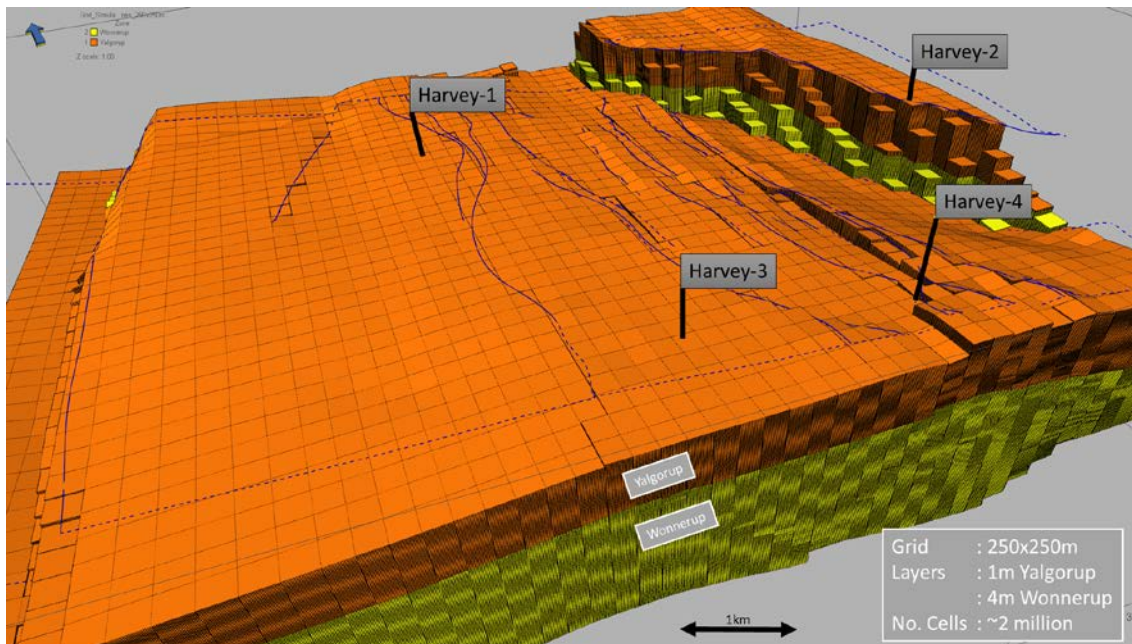


Figure 7.20: Grid at 250x250m cell size.

7.9 Facies modelling

The facies used in the modelling process was based on the core facies but simplified into five (5) facies: High and Low Energy Fluvial, and Paleosols, with some Overbank facies in the Yalgorup, and cemented zones (Figure 7.21).

The facies model in the Wonnerup Member was built in three steps:

1. The High-Energy Fluvial facies was distributed within the Paleosol background as channel objects.
2. The Low-Mid Energy Fluvial facies was distributed with overbank and barriers (cemented) associated with the channel bodies.
3. The two facies properties are then merged into one.

For the “Reference” case the percentage of the Paleosol facies was increased higher than observed in the GSWA Harvey 1 well. This approach was taken as the seismic reflectivity away from the GSWA Harvey 1 well suggests more heterogeneity with the presences of paleosols and/or diagenesis creating baffles within the Wonnerup Member.

The alternate “Homogeneous” case uses the percentage of sand/shale as observed in the GSWA Harvey 1 well producing a more massive ‘bland’ reservoir section devoid of any baffles. This was the “Reference” case during the GEN3 phase of modelling.

The facies were populated using estimated horizontal variograms due to the insufficient number of wells to generate meaningful values. There was also vertical proportion applied bases on the well data in order to ensure the packages of paleosols were replicated as seen in the wells (Figure 7.23).

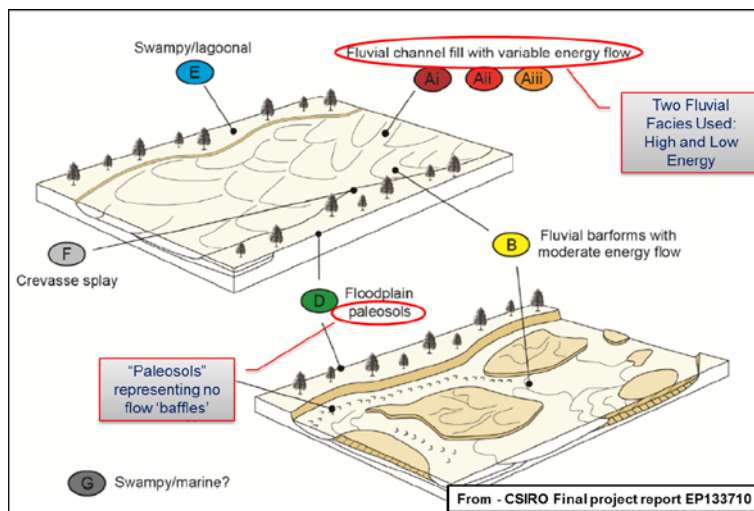


Figure 7.21: Simplified Facies types used in Facies Model

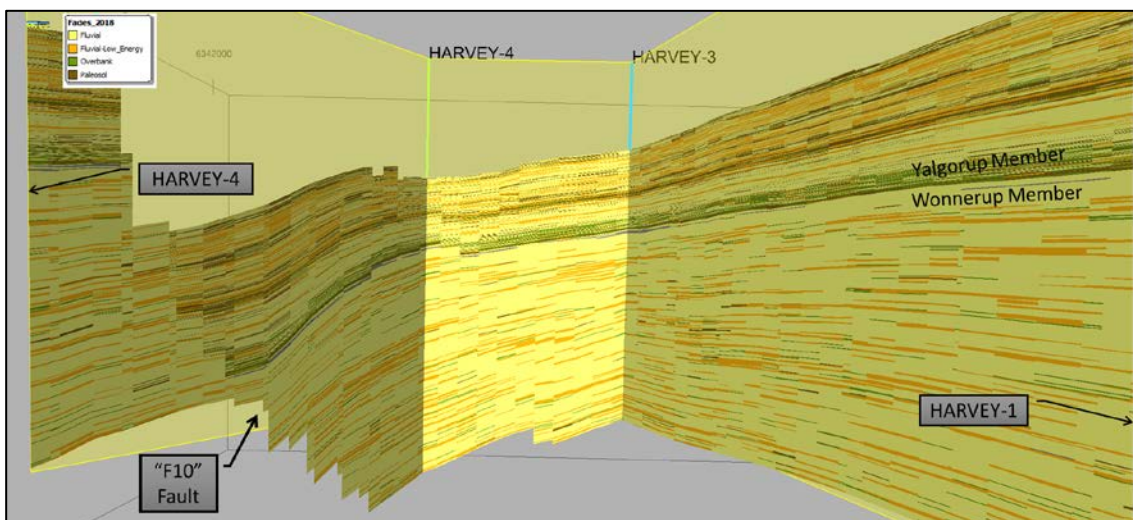


Figure 7.22: Section Showing the Facies Distribution

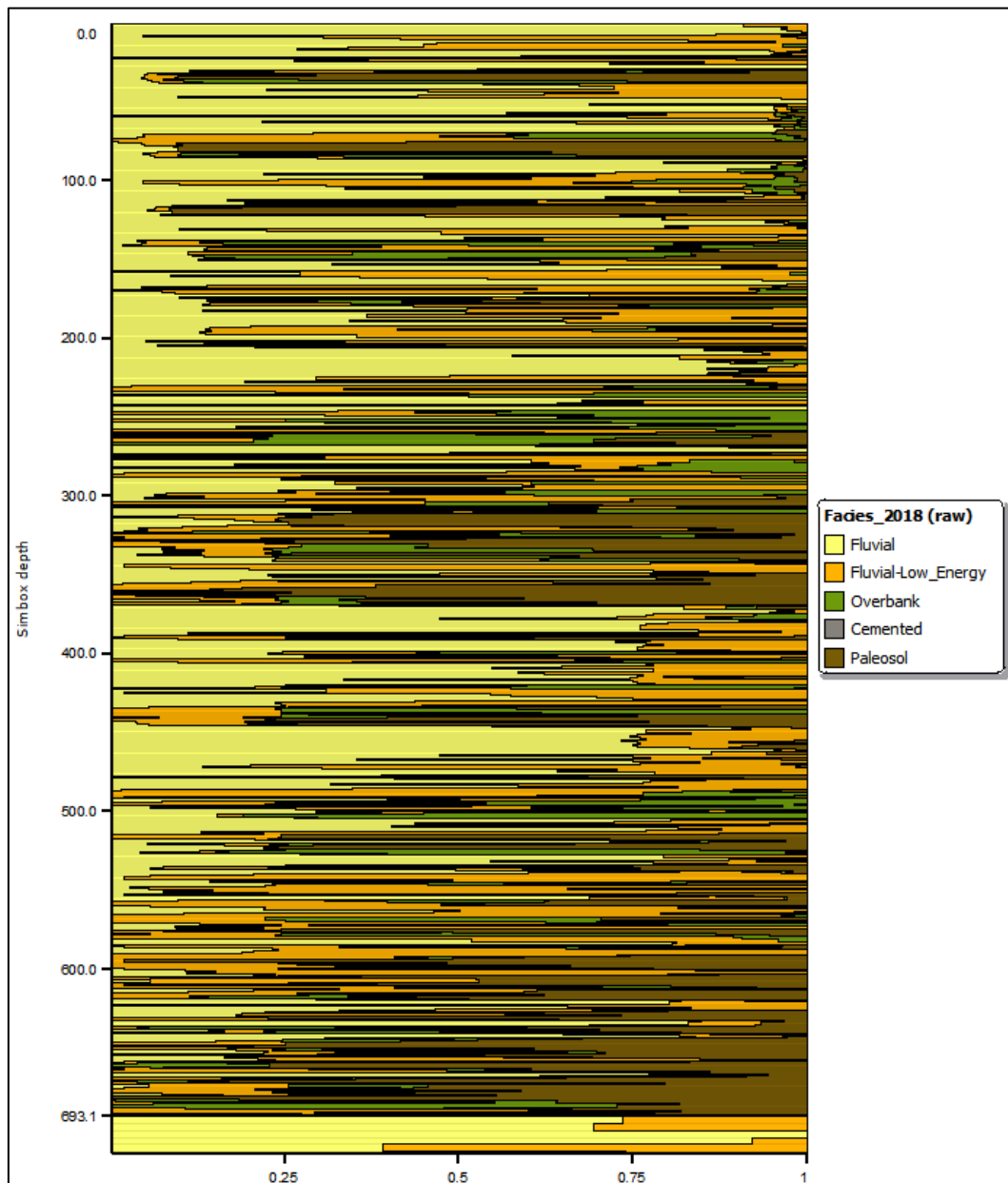


Figure 7.23: Vertical Proportions for Facies

7.10 Petrophysical modelling

In data analysis the logs were conditioned to the facies described in the previous section. Each portion of the facies curve as per corresponding facies was analysed and a best fit curve to describe the distribution assigned.

Porosity logs were scaled up into the 3D grid using arithmetic averaging. Porosity was then modelled across the grid using “Global Kriging” algorithm conditioned to the property

with an additional vertical trend applied (porosity depth trend shown in Figure 7.24). There are insufficient number of wells to generate meaningful sample horizontal variograms directly from the input data. Therefore, estimated anisotropic variograms were used to distribute porosity.

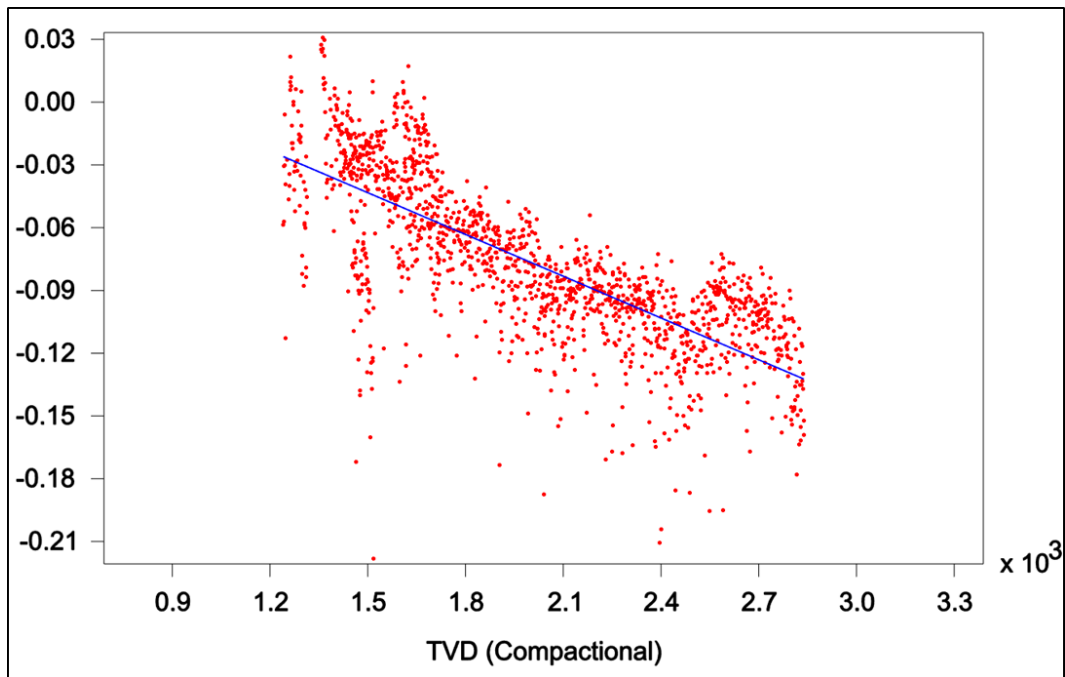


Figure 7.24: Porosity Depth Trend.

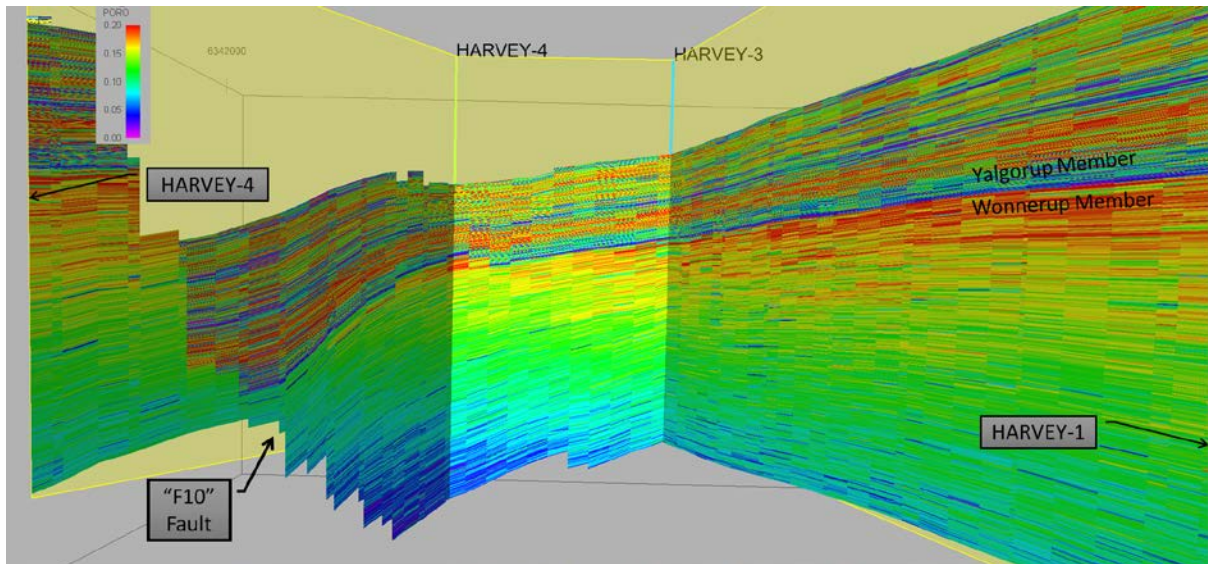


Figure 7.25: Section showing porosity distribution.

Permeability curves were derived by building a porosity to permeability transform based on all core and Nuclear Magnetic Resonance (NMR) data (Walker, 2017)ⁱ. This revised porosity to permeability transform (Figure 7.26) was applied to the porosity curve to create the permeability curve. The mean permeability derived using this transform is 138mD. This curve was then loaded into RMS and blocked to the grid cell size. The permeability was then distributed within the 3D grid using a kriging algorithm based on a correlation between permeability and porosity.

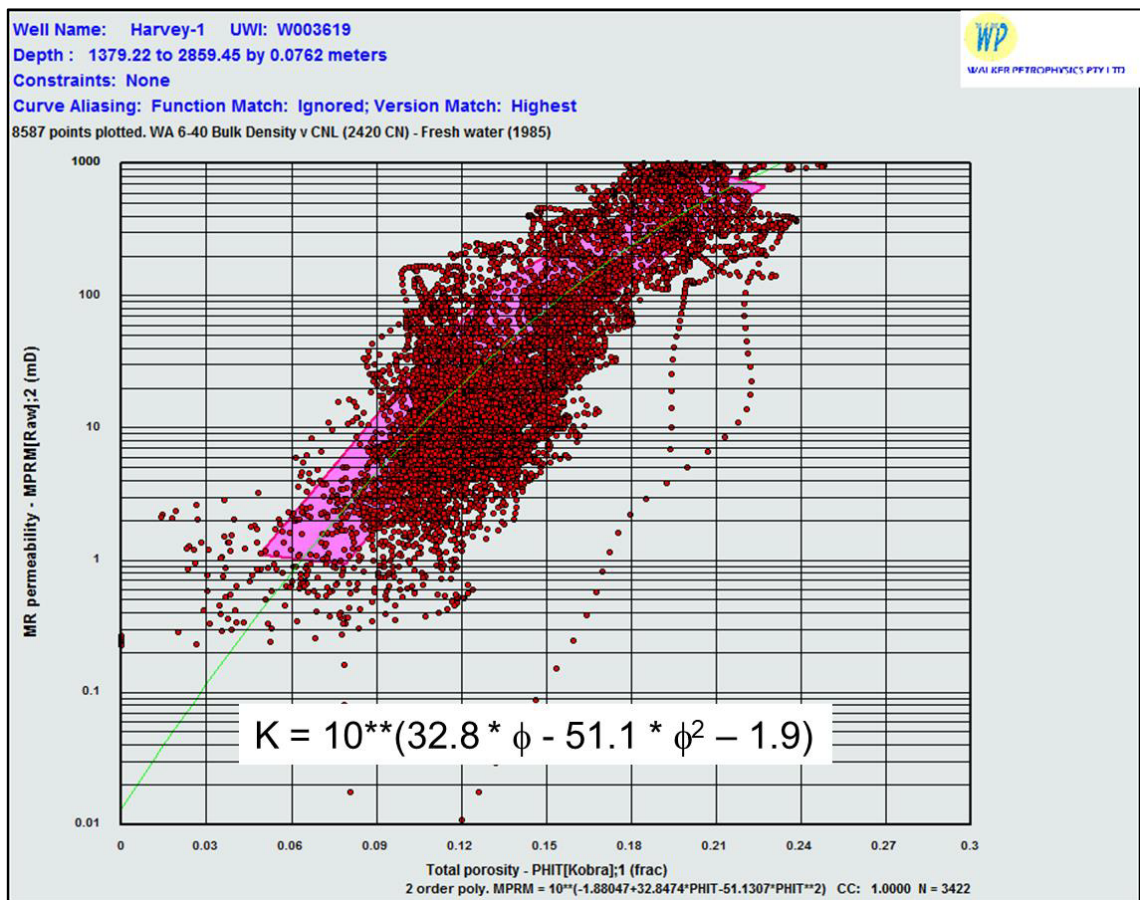


Figure 7.26: Revised Porosity Permeability Transform for Wonnerup

The previously generated permeability curves (Strachan, 2016)ⁱⁱ using porosity to permeability transform based only on the core available at the time, resulted in a permeability average of 200mD in the Wonnerup. The “High Perm” case during this phase of modelling (GEN4) was based on this previously derived permeability property with the average permeability of 200mD for the Wonnerup (Figure 7.27). This is the

ⁱ ODIN Report DMIRS/2018/2

ⁱⁱ GEN3 Modelling in 2016

equivalent of multiplying the permeability by 1.4 to produce the “High Perm” simulation case.

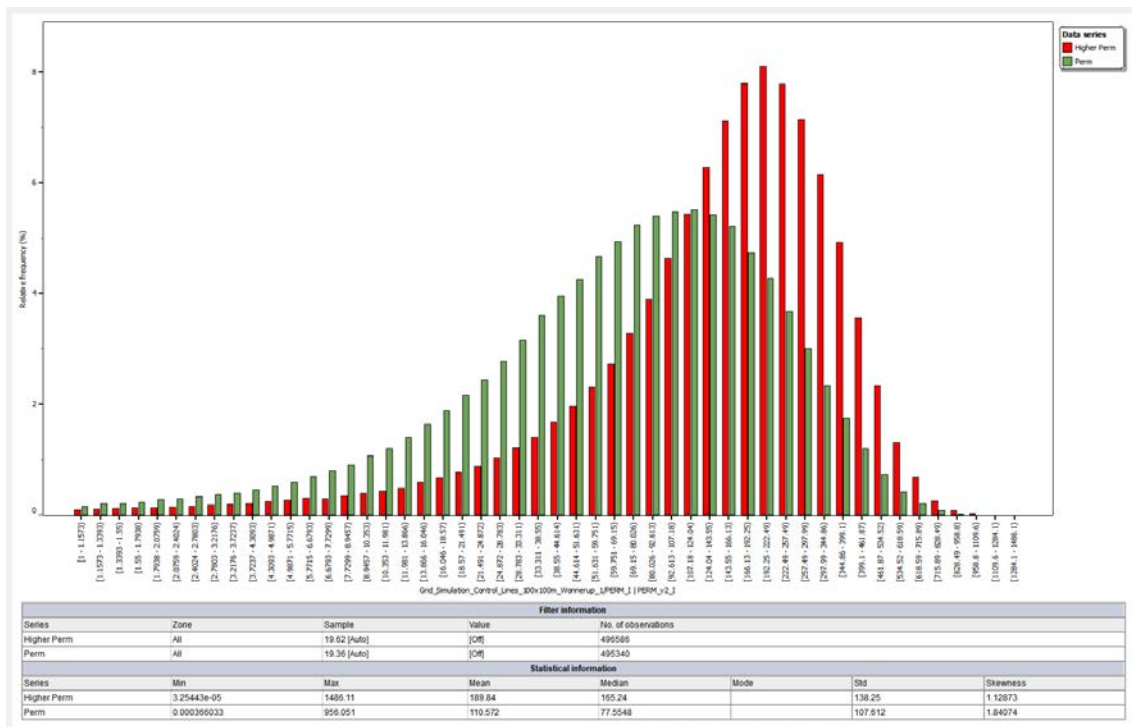


Figure 7.27: Permeability Distribution – “Reference” Versus “High Perm” Case

7.11 Sensitivity and uncertainty analysis

A number of subsurface uncertainties are discussed in this section and the impact of these uncertainty have been assessed during the model building process.

The key uncertainties identified of the static modelling are:

- How extensive are the individual paleosol geobodies?
- Porosity versus depth trend.
- Permeability range. The mean permeability for the Wonnerup based on the log data was 200mD for the previous GEN3 study and only 110mD for this study.
- Fault Seal Analysis was conducted during the GEN3 study, the results indicated very low chance of fault seal. However, a fault transmissibility of 0.01 was applied to access the impact of partially sealing faults.

- Kv/Kh will influence the flow of CO₂ in the reservoir. It is scale dependent, so care was taken during upscaling permeability, however, further sensitivity to varying Kv/Kh was also investigated during simulation by creating a vertical permeability equal to 0.1 times the horizontal permeability and 0.8 times the horizontal permeability.
- Impact of upscaling cells for simulation has been assessed.

The range of geological uncertainties investigated in the geomodelling study are summarised in Table 2. Geological models representing these ranges were incorporated into dynamic models investigating the movement of the CO₂ plume during injection of CO₂ and subsequent shut-in.

Table 2: Summary of ranges/scenarios for injection and/or plume migration

Parameter	Range (Gen 3 Models)	Range (Gen 4 Models)	Comments
<i>Paleosol Dimensions</i>	500-1500-3500m	300-3000-10000m	Based on an extension literature review and analogues a wider range of paleosol sizes have been used in Gen4.
<i>Permeability range in the Wonnerup</i>	71 to 372mD. Mean = 200mD	0 to 900 mD Mean = 138mD High Perm Case: Mean = 200mD	Significantly reduced permeability based on the NMR interpreted permeability and the porosity versus depth trend used.
<i>Fault Seal</i>	0.1 & 1	0.01 & 1	Open/partially closed system for internal faults.
<i>Fault Permeability</i>	x10	x10	Multiply vertical perm near faults by 10.
<i>Kv/Kh in the Wonnerup</i>	Mean = 0.3 to 1	0.1 x Horizontal & 0.8 x Horizontal Perm	
<i>Seismic Based Case</i>	Additional paleosols.	Reference Case	Seismic based case with higher concentration of paleosols/diagenesis in the Wonnerup.
<i>Homogeneous Case</i>	Reference Case	Homogeneous Reservoir or "Bland" Case	Lower percentage of paleosols in the Wonnerup.

8. CONCLUSION

The Harvey structure, onshore Perth Basin, is a North-South elongated fault bounded anticline. The study area for this project within this structure covers 332km² and is located approximately 13km northwest of the town of Harvey south of Perth. The static model grids built for this study are 10km wide by 12.5km long, covering an area of approximately 125km².

The static model study provided a reasonable description of the sub-surface in the Harvey area using the detailed interpretation of faults and horizons from seismic. The four Harvey wells are within the modelled area and incorporate the updated permeability log. Impact of upscaling cells for simulation has been assessed by comparing the plume migration through various grids with cell sizes of 25X25m, 50X50m, 100X100m and 250X250m. The 250X250m cell size was deemed to be a suitable representation of the broad plume migration and therefore used for sensitivity/uncertainty simulation runs (Lim, 2017).

A number of subsurface uncertainties were identified, and the impact of these uncertainties have been assessed during the model building process. These include;

- How extensive are the individual paleosol geobodies?
- Porosity versus depth trend.
- Permeability range. The mean permeability for the Wonnerup based on the log data was 200mD for the previous GEN3 study and only 110mD for this study.
- Fault Seal Analysis was conducted during the GEN3 study, the results indicated very low chance of fault seal. However, a fault transmissibility of 0.01 was applied to assess the impact of partially sealing faults.
- Kv/Kh will influence the flow of CO₂ in the reservoir. It is scale dependent, so care was taken during upscaling permeability, however, further sensitivity to varying Kv/Kh was also investigated during simulation by creating a vertical permeability equal to 0.1 times the horizontal permeability and 0.8 times the horizontal permeability.
- Impact of upscaling cells for simulation has been assessed.

The “Reference” case for this phase of modelling was aligned with the interpretation the seismic showing more heterogeneity within the Wonnerup Member than observed in the GSWA Harvey-1 well. However, a “Homogeneous” case replicating the reservoir

distribution observed in the GSWA Harvey-1 well produced a more massive ‘bland’ reservoir section devoid of any baffles. This was the “Reference” case during the previous GEN3 phase of modelling but is now referred to as the “Homogeneous” or “Bland” case in the current (GEN4) phase.

The other point of distinction between this phase of modelling compared to the previous GEN3 models was a greater degradation of porosity with depth. Thus, resulting in extremely low values of porosity (and therefore permeability) towards the base of the model. However, this did not impact the injectivity of the reservoir and did not appear to have any affect on the plume migration when compared to the previous modelling phase.

Geological models representing various sensitivities as listed above such as range of permeability, fault seal, fault permeability, vertical versus horizontal permeability and facies distribution were incorporated into dynamic models investigating the movement of the CO₂ plume during injection of CO₂ and subsequent shut-in period.

As shown in the ODIN Workflow (Figure 3.2), the learnings from the first phase of this project including “Advanced Seismic Interpretation” (Lamberto, 2017) , “Log Analysis” (Walker, 2017) , “Geology and Integration” (Strachan, et al., 2017) and previous studies have been applied to the study.

9. REFERENCES

1. **Beerbower, J.R. 1961.** Origin of cyclothems of the Dunkard Group (Upper Pennsylvanian-Lower Permian) in Pennsylvania, West Virginia, and Ohio. 1961, Vols. v. 72 p. 1029–1050.
2. **Fedorko, N., Skema, V. 2011.** *Stratigraphy of the Dunkard Group in West Virginia and Pennsylvania*. s.l. : Guidebook, 76th Annual Field Conference of Pennsylvania Geologists, Field Conference of Pennsylvania Geologists, Inc., Pennsylvania, p. 1–26., 2011.
3. **Herbert, C. and Uren, R. 1972.** *Duffys Forest shale deposit.-proposed drilling programme*. s.l. : Geological Survey New South Wales, 1972. Geological Survey New South Wales, Rpt. GS 1972.
4. **Kennedy, M. 2015.** *Petrophysical Interpretation of the Harvey Wells*. s.l. : ODIN Reservoir Consultants, 2015. DMP/2015/3.
5. **Kraus, M.J. 1999.** *Paleosols in clastic sedimentary rocks; their geologic applications*. : s.l. : Earth Science Reviews, 1999. Earth Science Reviews, v. 47, p. 41–70..
6. **Lamberto, John. 2017.** *Advanced Seismic Interpretation*. s.l. : ODIN Consultants, 2017. Report DMIRS/2018/1.
7. **Lim, David. 2017.** *Black Oil Modelling of CO2 Sequestration*. s.l. : ODIN Consultants, 2017. Report DMIRS/2018/5.
8. **Piane, Claudio Delle, et al. 2013.** *Facies-based rock properties distribution along the Harvey 1 stratigraphic well*. s.l. : CSIRO, 2013. CSIRO Final project report EP133710 June 2013.
9. **Roestenburg, J. 2016.** *The interpretation of image data for depositional facies orientation used in building a Static Model for the Harvey CO2 sequestration area*. s.l. : ODIN Reservoir Consultants, 2016. DMP/2016/2.
10. **Rust, Brian R. and Nanson, Gerald C. 1986.** *Contemporary and palaeo channel patterns and the late Quaternary stratigraphy of Cooper Creek, Southwest Queensland, Australia*. s.l. : Earth Surface Processes and Landforms., 1986. 11. 581 - 590. 10.1002/esp.3290110602. .
11. **Standard. 1969.** *Hawkesbury Sandstone, in Packham, G. H., ed., The Geology of New South Wales*. s.l. : Journal Geological Society Australia, 1969. Journal Geological Society Australia, v. 16, p. 407-415.
12. **Strachan, G. 2016.** *Static Model of the Harvey Area and evaluation of its potential for CO2 sequestration from a geological perspective*. s.l. : ODIN, 2016. Report DMP/2016/5.
13. **Strachan, Geoff and Bravo, Cristina. 2017.** *Geology Update and Integration Report*. s.l. : ODIN Consultants, 2017. Report DMIRS/2018/4.

14. **Walker, M. 2017.** *Log Analysis and Integration with Core Data.* s.l. : ODIN, 2017. Report DMIRS/2018/2..
15. **Zhan, Y. 2014.** *2D Seismic Interpretation of the Harvey Area, Southern Perth Basin, Western Australia.* s.l. : GSWA, 2014. GSWA Record 2014/7.